10-15-1984

Multiple determination of the optical constants of thin-film coating materials

D. P. Arndt

R. M.A. Azzam
University of New Orleans, razzam@uno.edu

J. M. Bennett

J. P. Borgogno

C. K. Carniglia

See next page for additional authors

Multiple determination of the optical constants of thin-film coating materials

D. P. Arndt, R. M. A. Azzam, J. M. Bennett, J. P. Borgogno, C. K. Carniglia, W. E. Case, J. A. Dobrowolski, U. J. Gibson, T. Tuttle Hart, F. C. Ho, V. A. Hodgkin, W. P. Klapp, H. A. Macleod, E. Pelletier, M. K. Purvis, D. M. Quinn, D. H. Strome, R. Swenson, P. A. Temple, and T. F. Thonn

The seven participating laboratories received films of two different thicknesses of Sc_2O_3 and Rh. All samples of each material were prepared in a single deposition run. Brief descriptions are given of the various methods used for determination of the optical constants of these coating materials. The measurement data are presented, and the results are compared. The mean of the variances of the Sc_2O_3 refractive-index determinations in the 0.40–0.75-nm spectral region was 0.03. The corresponding variances for the refractive index and absorption coefficient of Rh were 0.35 and 0.26, respectively.

I. Introduction

There are numerous applications for optical multilayer interference coatings in science and technology. In the past years sophisticated designs based on use of both absorbing and nonabsorbing coating materials have become commonplace. For economic reasons the process still most commonly used for the preparation of such systems is based on thermal evaporation in a vacuum. It is common knowledge, however, that films produced by this process in different laboratories (or indeed, in different deposition systems of the same laboratory) have different optical constants. This is because different deposition geometries and conditions give rise to different film structures and compositions.

For the design and manufacture of multilayers a good knowledge of the refractive indices and absorption coefficients of the coating materials is essential. It is, therefore, not surprising that there exist hundreds of papers devoted to determination of these parameters. It almost seems that every laboratory has its own favorite method.

The Optical Materials and Thin Films Technical Group of the Optical Society of America organized a Symposium on the Characterization of the Optical and Mechanical Properties of Optical Coating Materials[1,2] at the 1983 Annual Meeting of the Society in New Orleans. In conjunction with this symposium it seemed appropriate to hold a panel discussion on the measurement of the optical constants of absorbing and nonabsorbing thin films. The panel consisted of R. M. A. Azzam, J. M. Bennett, W. E. Case, C. K. Carniglia, J. A. Dobrowolski (Chairman), U. J. Gibson, H. A. Macleod, and E. Pelletier.

These letters link the participating groups of authors to the subsections of Section III:

A–D. P. Arndt, J. M. Bennett, V. A. Hodgkin, and P. A. Temple are with U.S. Naval Weapons Center, Physics Division, Michelson Laboratory, China Lake, California 93555.

B–R. M. A. Azzam and T. F. Thonn are with University of New Orleans, Department of Electrical Engineering, Lakefront, New Orleans, Louisiana 70148.

C–J. P. Borgogno and E. Pelletier are with École Nationale Supérieure de Physique, Centre d'Étude des Couches Minces, Domaine Universitaire de St. Jérôme, 13397 Marseille CEDEX 13, France.

D–C. K. Carniglia, T. Tuttle Hart, W. P. Klapp, and D. M. Quinn are with Optical Coating Laboratory, Inc., 2789 Northpoint Parkway, Santa Rosa, California 95407-7397.

E–W. E. Case, M. K. Purvis, and D. H. Strome are with LTV Aerospace & Defense Company, Vought Missiles & Advanced Programs Division, P.O. Box 225907, Dallas, Texas 75265.

F–J. A. Dobrowolski and F. C. Ho are with National Research Council of Canada, Division of Physics, Ottawa, Ontario, K1A 0R6.

G–U. J. Gibson and R. Swenson are with University of Arizona, Optical Sciences Center, Tucson, Arizona 85721.

H–H. A. Macleod and R. Swenson are with University of Arizona, Optical Sciences Center, Tucson, Arizona 85721.

Received 11 May 1984.

The intention of the panel discussion was to demonstrate that, even for nominally the same films, careful experimenters will obtain different values of the optical constants, depending on the method used and the model assumed for the films. To this end the panelists were asked to use their favorite method to determine the optical constants from two samples each of one metallic and one dielectric coating material supplied to them. They were requested to give a brief description of their method and to present their results in graphical or tabular form during the panel discussion. These results, and their intercomparison, resulted in a lively discussion. Many members of the audience requested that this work be made available in *Applied Optics*. This was made possible through the generous cooperation of the panelists and their colleagues.

It may be of interest to state briefly how this paper was written. Because it was deemed desirable that the contributions from the various laboratories cover the same ground, a brief set of instructions was prepared. Among other things, it was suggested that reference be made to a published description of the method with only a skeleton outline in the present text. Only if this were not possible should an adequate, but laconic, description be given. The thin-film model and assumptions used in the calculations were to be clearly stated. The apparatus used, cleaning procedures employed, and the conditions prevailing during the measurements were to be described. Whenever possible, raw measurement data were to be included. Results were to be presented in graphical or tabular form together with an estimate of the sensitivity of the determination. The perceived advantages and disadvantages of the method were to be stated.

The paper was prepared for publication by J. A. Dobrowolski, who also wrote Secs. I and IV. C. K. Carniglia provided Sec. II. The texts from the participating groups were edited only to standardize nomenclature, units, and format. They are presented in Sec. III.A–III.H. (The letters A–H correspond to the groups in the byline.) The symbols adopted for this paper are defined in Table I. Some tables were merged, and one or two figures with data that also appeared in tabular form were omitted to reduce the length of the paper. Most figures were redrawn. The resulting manuscript was submitted to all participating laboratories for corrections and approval.

Table I. Terminology Used in This Paper

λ	- wavelength (nm)
t	- thickness of film (nm)
n_0, n_s	- refractive index of air, substrate
n, n_1, n_i	- film refractive indices: average, and at air, substrate interfaces
Δn	- inhomogeneity of film refractive index
k	- film absorption coefficient
A, A'	- film absorption for front, back surface incidence of light
T_w, R_w	- transmittance, reflectance of uncoated witness
$R_{w,c}$	- as above, but calculated value
T_s, R_s	- transmittance, reflectance of single, uncoated surface of substrate
T, R, R'	- transmittance, front- and back surface reflectances of coated substrate with second surface reflections
T_c, R_c, R'_c	- as above, but calculated values
T_f, R_f, T'_f	- transmittance, front- and back surface reflectances of film on substrate without second surface reflections
T_{obs}	- T/T_w
T^*	- transmittance of coated substrate with uncoated witness oiled on
ϕ	- angle of incidence (°)
$T_p(\phi)$, $R_p(\phi)$	- transmittance, reflectance for light incident at ϕ° and polarized parallel to plane of incidence
$T_s(\phi)$, $R_s(\phi)$	- as above, but for light polarized perpendicular to plane of incidence
T_{max}, T_{min}	- transmittance at maximum, minimum
R_{max}, R_{min}	- reflectance at maximum, minimum
T_{int}	- maximum transmittance interpolated to position of minimum
Δ, Ψ	- ellipsometric angles

II. Sample Preparation

The substrates used for the coatings were 38.6-mm (1.52-in.) diam by 3-mm (0.12-in.) thick Dynasil (fused silica) commercially polished to an 80/50 finish on both sides. Highly polished surfaces (bowl-feed polished, for example) would have provided better cosmetic quality—especially for the metal films—but they were not used, for reasons of economy and time, and because it was felt that commercially polished surfaces were more representative of standard laboratory practice. The dispersion curve for fused silica is given by

$$n_s^2 - 1 = \frac{0.69617\lambda^2}{\lambda^2 - 0.0046792} + \frac{0.40704\lambda^2}{\lambda^2 - 0.013512} + \frac{0.89748\lambda^2}{\lambda^2 - 97.93}, \quad (1)$$

for wavelengths measured in micrometers.[3] The transmittance of the Dynasil substrate was measured and found to agree with the values expected from the published dispersion curve to within 0.2% over the 300–900-nm range. At wavelengths shorter than 300 nm there is slight absorption with the beginning of the absorption edge in evidence at 220 nm. The substrates for the dielectric films measured by CECM[C] were provided by their laboratory and were 3.5 × 7 cm with a 15° wedge between the surfaces. All parts were cleaned using detergent and deionized water and then exposed to alcohol vapors to remove residual water.

The films were prepared in a diffusion-pumped box coating chamber measuring 1.2 m on a side. The parts were held in racks in a double-rotation planetary system. All the 38.6-mm parts of a given material and thickness were held in a single rack, while the corresponding CECM part was in a similar rack in the same run. Rack-to-rack variations in thickness were expected to be <1%. The variation in thickness over the surface of a part was measured for one of the dielectric films and found to be <0.5%. Thickness variation among parts in the same rack was expected to be negligible.

The dielectric coating material selected for this study was scandium oxide (Sc_2O_3). The material was Cerac spectroscopic grade, 325 mesh powder of 99.99% purity. This material has been used in the study of UV laser coatings, where it has proven to be relatively damage resistant.[4] The Sc_2O_3 was evaporated from an electron gun source. The coating temperature was 150°C—one of the temperatures used in the laser coating study.[4]

For the metal coating, rhodium (Rh) was used.[5] This metal is inert, so changes due to oxidation should be minimal. The Rh was from Cerac, 200 mesh of 99.9% purity, and was coated from a resistance source at ambient temperature. No adhesion or nucleation layers were used with the Rh because of the possible effect on the n and k values of the films. As a result, the films were relatively fragile and difficult to clean. Auger analysis of the metal films verified that they were Rh and did not show appreciable amounts of oxygen or carbon.

Coatings of two different thicknesses were made for each material. In each case, the thicker film was to be approximately twice as thick as the thinner one. Having two coatings with a known thickness ratio is helpful in the data analysis. For the metal coatings, the additional data act as a check against spurious solutions for n, k and thickness. For the dielectric coatings, the 2:1 ratio provides halfwave points from the thicker sample at quarterwave points of the thinner sample, again allowing for improved analysis techniques. An optical thickness of approximately three quarterwaves at 550 nm was chosen for the thinner Sc_2O_3 coating. This, together with the thicker six-quarterwave sample, provided several turning points throughout the visible and near UV region of the spectrum. The thinner of the Rh samples had a transmittance of 0.18 at 550 nm. This value was chosen so that the film would be thick enough to have well-defined optical properties yet allow a film twice as thick to still be slightly transparent (T = 0.07).

All the dielectric coatings were made in a single run. Two racks of 38.6-mm parts and two racks with the CECM parts were included. The coating thickness was determined using a previously calibrated optical monitoring system. The two different thicknesses were achieved using movable masks. All the parts were coated with the thinner of the two films. After this film was complete, the evaporation was interrupted while the movable masks were used to cover one set of the 38.6-mm parts and one of the CECM parts. The evaporation was then continued using a fresh monitor chip, and a coating of identical thickness was deposited onto the remaining parts. Any deviation from a 2:1 thickness ratio would presumably be due to differences between the nucleation of the film material on the substrate and its nucleation on itself. These differences were expected to be small. A similar procedure was used for the coating of the Rh films, except that there were no CECM parts in the run.

It was desirable to include a sharp edge or step at some point on the film to facilitate thickness measurements by mechanical profiling instruments. This step in film thickness was required to be near the edge of the film so that optical measurements would not be obstructed. The step was achieved by pressing a thin tab of beryllium copper against the face of the part near one edge during the coating process. This small mask, which protruded ~7.6 mm (0.3 in.) in from the edge of the substrate, provided a sharp edge between the uncoated and coated portions of the substrate.

After being coated, the 38.6-mm parts were placed into specially machined plastic shipping containers with lids which were recessed, so that the face of each part was contacted only in a narrow ring near the edge. The containers were sealed with plastic tape to keep out dust. Four coated parts—a thick and a thin sample of each material—together with an uncoated witness were shipped to each laboratory for measurement.

III. Determination of the Optical Constants

A. *R, T, t* Method

The optical constants of the Sc_2O_3 and Rh films were calculated from measurements of the film thickness, normal incidence reflectance R, and transmittance T. Two different instruments were used for the R and T measurements.

A 50-mW Spectra-Physics model 171-19 argon-ion laser with a beam diameter of ~2 mm was used to measure T at normal incidence and R at 1° incidence at wavelengths of 488.0 and 514.5 nm. Each film-coated sample had an additional fused quartz substrate oiled onto the back surface using an index matching fluid to eliminate interference effects of the laser beam in the 3.2-mm (0.125-in.) thick substrate. Both R and T were determined as ratios of sample-in to sample-out of the beam in the single beam instrument (see Table II). To eliminate the effect of source fluctuations, two Laser Precision pyroelectric detectors ratioed the signal from the sample, or from the beam at the sample position, to the incident beam. The precision (repeatability) of the R and T measurements was a few parts in the fourth decimal place, while the accuracy was approximately ±0.001.

Normal incidence transmittance was also measured at eight wavelengths in the 450–800-nm wavelength range as the ratio of T, the film-coated sample transmittance, to T_w, the transmittance of an identical uncoated fused quartz substrate. The film-coated and uncoated substrates were alternately placed in front of the entrance slit of a spectrophotometer designed to measure the change in reflectance with temperature.[6] The instrument had Perkin-Elmer Corp. source optics (tungsten source) and a P-E model 99 double-pass monochromator with a potassium bromide prism disperser. Since the source optics module was enclosed, the sample and bare substrate became slightly heated, but the temperature was not measured. The standard deviation of the twelve ratio measurements made at each wavelength was ~0.06% of the Sc_2O_3 ratio and ~0.03% of the Rh ratio. Since the ratios were quite different for the two materials (see Table III), the absolute values of the standard deviations differed accordingly. The accuracy of the measurements was probably better than 0.1% and included factors such as the linearity of the detector and electronics and the wavelength calibration. All the measurements were made with the samples in room air.

Before the Sc_2O_3 samples were measured, they were drag wiped once using Kodak lens tissue moistened with methanol (gas chromatography grade). An attempt was made to drag wipe the thick Rh sample, but the film became badly scratched. Fortunately we were able to obtain the sample that had been measured at OCLI.

The normal incidence reflectance of the samples was not measured at NWC, except at the two argon wavelengths, because the absolute reflectometer[7] was not in operation. However, OCLI kindly provided absolute reflectance data for the Rh films measured on a Cary 17D spectrophotometer using a V-W attachment. Details of the measurements are given in Sec. III.D. The Rh films appeared to contain pinholes and possibly particulate contamination when observed under Nomarski illumination. These defects were avoided as much as possible when making the optical measurements described above.

Thicknesses of all four films were measured on a Talystep surface profiling instrument[8] at three positions

Table II. *R, T* and *t* Method: Measurements of Optical Constants Using an Argon-Ion Laser

Material	t (nm)	λ (nm)	Transmittance T	Transmittance T_f	Reflectance R	Reflectance R_f	R + T	n	k
Sc_2O_3	224.5	488.0	0.8397	—	0.1556	—	0.9953		
		488.0	0.8444‡	0.8713	—	—	1.0000	1.82*	0
		514.5	0.8168	—	0.1805	—	0.9973		
		514.5	0.8195‡	0.8446	—	—	1.0000	1.90*	0
Sc_2O_3	452.5	488.0	0.8052	—	0.1923	—	0.9975		
		488.0	0.8077‡	0.8323	—	—	1.0000	1.872	0
		514.5	0.8630	—	0.1359	—	0.9989		
		514.5	0.8641‡	0.8921	—	—	1.0000	1.854	0
Rh	14.2	488.0	0.1924	0.1963	0.4405	0.4391	0.6329	1.80	3.551
		514.5	0.1638	0.1671	0.4417	0.4407	0.6055	2.45	3.582
Rh	27.1	488.0	0.0498	0.0506	0.5452	0.5451	0.5950	3.24*	3.09*
		514.5	0.0654	0.0664	0.5639	0.5637	0.6293	2.18	3.438

* Compromise solution
‡ Value of T increased to make R + T = 1 (see text)

All films were measured on 9/26-27/83 except for the thick Rh film which was measured on 10/7/83.

along the 12.7-mm (0.5-in.) long masked region near the edge of each sample. A 2-mg stylus loading was used to obtain a nondestructive measurement of the step. This loading was previously found to not leave permanent marks on films of the type measured here. The results are as follows:

Sc_2O_3 (thick) 452.5 ± 1.4 nm, Rh (thick) 27.1 ± 1.4 nm,
(thin) 224.5 ± 0.7 nm, (thin) 14.2 ± 1.7 nm.

The uncertainties in the Sc_2O_3 film thicknesses are primarily caused by the 3.27 and 1.63-nm digitization increments of the profile data for the thick and thin films plus small actual thickness variations between the three places measured. (Two measurements were made at each place.) The uncertainties in the Rh film thicknesses are caused by the ~3.5-nm peak-to-valley roughness of the commercially polished fused silica substrates. The height calibration of the Talystep instrument was checked at the time of the measurements using a 702.2-nm thick Ge film that had previously been measured on a FECO interferometer.[9] The instrument calibration was found to be good to ~0.2% of the total film thickness. The thin Sc_2O_3 and Rh films were intended to be half as thick as the thick films of the same materials. This is certainly true for the Rh films and probably also true for the Sc_2O_3 films, although the difference is outside the quoted uncertainties.

The measured R and T data for all films and also the calculated optical constants are shown in Tables II and III. Table II contains measurements taken with the argon-ion laser, while Table III includes NWC transmittance data and OCLI reflectance data taken on spectrophotometer-type instruments. (The OCLI data are from a continuous wavelength scan while the NWC measurements were taken point by point.) In Table II the columns labeled T and R are the measured quan-

Table III. *R*, *T* and *t* Method: Measurements of Optical Constants Using Spectrophotometer-type Instruments

Material	t (nm)	λ (nm)	Transmittance‡ T/T_w	Transmittance‡ T_f	R_f‡‡	R_f+T_f	n	k
Sc_2O_3	224.5	450.0	0.9512	0.9157	—	—	1.700	0
		488.0	0.9054	0.8704	—	—	1.82*	0
		500.0	0.8923	0.8576	—	—	1.860	0
		514.5	0.8857	0.8510	—	—	1.864	0
		550.0	0.8749	0.8406	—	—	1.844	0
		600.0	0.8903	0.8561	—	—	1.842	0
		650.0	0.9273	0.8930	—	—	1.836	0
		700.0	0.9646	0.9303	—	—	1.828	0
		750.0	0.9903	0.9560	—	—	1.817	0
		800.0	1.0004	0.9663	—	—	1.780	0
Sc_2O_3	452.5	450.0	0.9276	0.8922	—	—	1.860	0
		488.0	0.8913	0.8564	—	—	1.832	0
		500.0	0.8993	0.8645	—	—	1.848	0
		514.5	0.9273	0.8923	—	—	1.854	0
		550.0	0.9925	0.9575	—	—	1.866_5	0
		600.0	0.9540	0.9193	—	—	1.863	0
		650.0	0.8847	0.8507	—	—	1.816_5	0
		700.0	0.8925	0.8586	—	—	1.836_4	0
		750.0	0.9448	0.9107	—	—	1.840	0
		800.0	0.9875	0.9535	—	—	1.851	0
Rh	14.2	450.0	0.1728	0.1643	0.4367	0.6010	2.40	3.28_5
		500.0	0.1756	0.1671	0.4322	0.5993	2.60	3.40
		550.0	0.1769	0.1684	0.4311	0.5995	2.78	3.53
		600.0	0.1779	0.1694	0.4294	0.5988	2.95	3.65
		650.0	0.1790	0.1705	0.4284	0.5989	3.11	3.77
		700.0	0.1800	0.1715	0.4282	0.5997	3.23	3.91
		750.0	0.1812	0.1726	0.4272	0.5998	3.35	4.03
		800.0	0.1827	0.1741	0.4265	0.6006	3.42	4.17_5
Rh	27.1	450.0	0.0589	0.0557	0.5597	0.6154	2.27	3.25_3
		500.0	0.0627	0.0594	0.5649	0.6243	2.39	3.41_5
		550.0	0.0653	0.0618	0.5698	0.6316	2.51	3.58
		600.0	0.0672	0.0636	0.5745	0.6381	2.62	3.74_5
		650.0	0.0689	0.0652	0.5770	0.6422	2.75	3.88_9
		700.0	0.0702	0.0665	0.5797	0.6462	2.87	4.03_5
		750.0	0.0714	0.0677	0.5808	0.6485	3.01	4.15_9
		800.0	0.0726	0.0688	0.5820	0.6508	3.14	4.28

* Compromise solution
‡ Transmittance values measured at NWC on 10/12-14/83
‡‡ Reflectance values measured at OCLI on 9/30/83

tities for each sample, which include the effect of the back surface of the substrate and multiple reflections within the substrate. The columns labeled T_f and R_f are the corrected values of transmittance or reflectance from air, through the film, and into the substrate. These are used in the calculations of optical constants, as discussed in the next section. The measured sample reflectance and transmittance are summed in the column labeled $R + T$. The sum for the Sc_2O_3 films is nearly unity, indicating that the residual absorption and scattering losses are small. The reflected scattering into a hemisphere was measured at a wavelength of 514.5 nm for these two films using the Optical Evaluation Facility (OEF)[10]; the hemispherical scattering was 2.9×10^{-4} of the incident beam intensity, about an order of magnitude smaller than the differences from unity given in Table II. Because of the small depth of focus in the OEF, the measured scattering primarily occurred in the film. Some scattering could be seen in the index matching fluid when the samples were illuminated by the argon-ion laser. Scattering and absorption in the index matching fluid could probably account for all the difference from unity of the $R + T$ values. Thus the Sc_2O_3 films were assumed to be nonabsorbing and homogeneous, and the transmittance values were increased to make $R + T = 1$ in the calculations of the optical constants. The second entries in the T column at each wavelength give these values.

In Table III the columns under Transmittance give T/T_w and T_f as previously mentioned. In the measured OCLI reflectance data R_f for the Rh films, the effect of the back surface of the substrate has been neglected.

The measured data for the Sc_2O_3 films were corrected and the optical constants were calculated as follows. Since k was assumed to be zero, n could be calculated from the measured transmittance and film thickness; reflectance data are not needed. To obtain T_f without the effect of the back surface of the substrate and multiple reflections within the substrate, the T values in Table II were corrected using Eq. (16) in Ref. 11:

$$T_f = T(1 - R_f' R_s)/T_s, \tag{2}$$

where T_s and R_s are the air–substrate transmittance and reflectance for a bare single surface. Here T_f was calculated twice using, first, a value of $1 - T$ for R_f and, second, the $1 - T_f$ value from the first calculation. To calculate T_f from T/T_w in Table III, the latter values were multiplied by the calculated transmittance T_w of an uncoated fused silica sample, taking into account both surfaces and multiple reflections within the sample. The value of T_w was calculated from Eq. (15) in Ref. 11; refractive-index values for fused silica were obtained from the *AMERICAN INSTITUTE OF PHYSICS HANDBOOK*.[3]

The Rh transmittance values T/T_w in Table III were first multiplied by T_w as for the Sc_2O_3 films. Then T in both tables was changed to T_f using Eq. (11) from Ref. 6:

$$T_f = T_{obs}(1 - R_s + R_s A_f')/[1 + R_s(1 - T_{obs})], \tag{3}$$

where T_{obs} is T/T_w, and A_f' is the absorption in the film. (Actually A_f' is the absorption in the film when light is incident on the film from the substrate side. However, since T_f is so close to T_{obs}, the small difference between A_f and A_f' is negligible.) Since A_f is equal to $1 - T_f - R_f$ and T is nearly equal to T_f, T can be used in place of T_f to calculate A_f. No correction was necessary for the Rh reflectance data in Table III since R_f was measured directly. In Table II, the approximate relation

$$R_f = R - T_f^2 R_f \approx R(1 - T_f^2) \tag{4}$$

was used to correct the R values of the Rh films. Since the difference between R and R_f was very small, only ~ 0.001, R_f in the second term on the right-hand side of Eq. (4) was assumed to equal R. The differences between T and T_f for the thin and thick Rh films were also only a few tenths of a percent.

An iterative approach was used to obtain n and k for the Rh and n for the Sc_2O_3 films. Equations similar to the form given by Hass on p. 6-120 of Ref. 3 were programmed into a Hewlett-Packard calculator. Guesses were made for n and k; T_f and also R_f (for the Rh films) were calculated and compared with the measured quantities. The values of n and k were adjusted until the calculated and measured quantities agreed within the limits of experimental error, and the results are given in Tables II and III. In some cases (asterisks) exact solutions were not possible, probably because of inhomogeneities in the films, so compromise solutions are given where the fits are closest for both n and k.

The optical constants calculated for the Sc_2O_3 films show more variation than might be expected or desired. Specifically, the optical constants determined with the argon laser (Table II) do not agree for the two films and do not agree with values calculated from the spectrophotometer measurements in Table III. The optical constants for the two films in Table III do not agree with each other and, furthermore, have different wavelength dependences. Comparing the T_f values in Tables II and III for the two Sc_2O_3 films at 488.0 and 514.5 nm, it is seen that two of the values agree almost exactly, but the two others differ by more than the combined assumed errors in the measurements. The worst agreement is for the 452.5-nm thick Sc_2O_3 film at 488.0 nm where the T_f values differ by 0.0241. A possible explanation for these discrepancies is that the films are inhomogeneous—the optical constants may vary as a function of distance from the substrate or spatially across the substrate or both. Since different areas of the films were illuminated in the two instruments, spatial variations in film homogeneity could account for some of the observed effects. However, the fact that no single value of n could be used to predict the measured transmittance at 488.0 nm for the thinner film suggests that there is at least some inhomogeneity as a function of depth within the film. Another possible contributing factor would be a variation in film thickness as a function of position on the film, at least to the extent that it was different in the center where the transmittance was measured and at the edge where the thickness was measured. Spatial variation measurements were made at a wavelength of 488.0 nm on the

Table IV. *R*, *T* and *t* Method: Measurements on the 14.2-nm Thick Rh Film Using the Argon Laser; $\lambda = 488.0$ nm

Date	T	R	R + T	Position
9/27/83	0.1924	0.4405	0.6329	Center
10/14/83	0.1773	0.4362	0.6135	Center
10/14/83	0.1763	0.4432	0.6195	2 mm off center
10/14/83	0.1622	0.4255	0.5877	4 mm off center

thick Sc_2O_3 film using the argon laser. The value of $R + T$ varied by a maximum of only 0.005 over a 4-mm distance on the film.

The optical constants calculated for the Rh films also show some inconsistencies. However, in Table III the values of n and k increase with increasing wavelength for both films as well as in Table II where solutions for n and k were found. Note that the $R_f + T_f$ values for the thinner Rh film are nearly independent of wavelength, whereas they increase with wavelength for the thicker film. The absolute magnitude of $R_f + T_f$ is larger for the thicker film, meaning that the absorption, $1 - R_f - T_f$, is smaller. This latter conclusion is somewhat uncertain since the measurements were made on different thin Rh films but the same thick Rh film (although at different times). Also, aging effects were observed, as noted below.

Aging effects and spatial variations in the film properties were observed in the argon laser measurements on the thinner Rh film, as shown in Table IV. These indicate that not only is the absorption changing with time but also there is a short range spatial variation of the absorption. Further measurements should be made to determine if this effect is general for Rh or simply a one-time occurrence for this particular film. With a precise instrument, variations of 0.02 such as seen here should be easily measured.

In conclusion, the advantage of the normal incidence R, T, and film thickness method is that high accuracy, $\sim \pm 0.001$, optical measurements can be made with a minimum of systematic errors, and the mechanical film thickness can be measured with a small percentage error as long as the substrates on which the films are deposited are smooth compared with the film thickness. The method cannot give information about film inhomogeneities unless additional assumptions are made. Either a solution for n and k is obtained which fits the measured data, or it is not. With a small diameter laser beam as an illuminating source, differences in film properties can easily be detected as a function of position on the sample.

B. Reflection Ellipsometry

In ellipsometry[12] measurements of the polarization states of collimated monochromatic light before and after reflection from a surface permit determination of the ratio, $\rho = R_p/R_s = \tan\psi \exp(i\Delta)$, of the complex p and s reflection coefficients. A model of the reflecting sample is assumed (in the present case a homogeneous isotropic film with plane-parallel boundaries on a semi-infinite homogeneous and isotropic substrate), and the ratio of reflection coefficients is also computed. Model parameters (film complex refractive index $n - ik$ and thickness t) are sought (and found) that best match the computed and measured values of ρ.

Two-zone null measurements[13] were taken on a Gaertner L119XUV ellipsometer with a He–Ne laser ($\lambda = 632.8$ nm) and also with a Hg/Xe-arc lamp filtered by a GS100 Schoeffel monochromator (1-mm slit width = 8.5 nm) to pass a few visible wavelengths ($\lambda = 404.7$, 486.1, and 546.1 nm). At these wavelengths the Babinet-Soleil compensator settings for quarterwave retardation were already known. Measurements were made on all the samples as received (with no further cleaning) and in air.

To test the utility of multiple-angle-of-incidence ellipsometry (MAIE) for the determination of n, k, and t of the same film, data were initially taken on each sample at incidence angles $\phi = 40$ and 80° with $\lambda = 632.8$ nm. Having found that inversion of the ellipsometric equations using MAIE (2-ϕ) data is inferior to inversion based on ($2 - t$) data obtained on the two different-thickness films of the same material, all subsequent measurements, at all other wavelengths, were made at $\phi = 60°$ only.

For the bare fused silica substrate a pseudocomplex refractive index $\bar{n}_s - i\bar{k}_s$ was determined at each wavelength by ellipsometry. The value of n was consistently slightly less (by 0.01) than the corresponding value obtained by Malitson[14] using a prism refraction method, and $\bar{k}_s$, which does not represent any real absorption, was generally <0.005. The Brewster angle of the fused silica substrate was also measured, and its tangent agreed with Malitson's index to within two decimal places at all wavelengths. The pseudocomplex refractive index $\bar{n}_s - i\bar{k}_s$ accounts for the effect of the presence of a polish layer and roughness on the surface of fused silica and is, in principle, the preferred index to use in subsequent inversion of the ellipsometric equations to obtain film properties. However, all indices mentioned above differ only very little numerically, and all lead to essentially the same film parameters.

The two-zone-averaged values of ψ and Δ measured at the central region of the thin and thick Sc_2O_3 and Rh films are given in Table V.

Besides assuming that each film is homogeneous and isotropic and has plane-parallel boundaries, the thin and thick films of the same material (Sc_2O_3 or Rh) were presumed to have the same optical constants n and k. Film thicknesses are independently determined from ellipsometric data. The inversion method is an adaptation of one previously described.[15]

Table V. Reflection Ellipsometry Method: Ellipsometric Angles ψ and Δ (in degrees) of the Thin and Thick Sc_2O_3 and Rh Films and the Resulting Optical Constants

Material	λ (nm)	ϕ(°)	Thin Film ψ	Thin Film Δ	Thick film ψ	Thick film Δ	n	k
Sc_2O_3	404.7	60	12.85	93.41	14.285	116.08	2.07	0
	486.1	60	9.62	163.28	8.305	167.75	1.96	0
	546.1	60	7.425	205.37	10.77	113.33	1.85	0
	632.8	40	28.3675	187.89	30.6875	177.945	1.81	0
		80	32.9925	355.995	28.9125	356.045		
Rh	404.7	60	30.36	148.37	33.885	143.07	2.11	3.01
	486.1	60	29.64	154.27	33.775	148.69	2.51	3.21
	546.1	60	29.49	157.13	33.985	151.93	2.72	3.40
	632.8	40	39.2375	174.635	40.94	172.49	3.03	3.65
		80	15.865	68.43	23.65	84.38		

Table VI. Reflection Ellipsometry Method: Thicknesses of Rh Thin Films Independently Determined at Each Wavelength

λ (nm)	t_1 (nm)	t_2 (nm)	t_2/t_1
404.7	15.7	32.7	2.08
486.1	15.5	31.8	2.05
546.1	15.2	30.8	2.03
632.8	15.5	31.3	2.02
Averages	15.5 ± 0.2	31.6 ± 1.0	2.05 ± 0.03

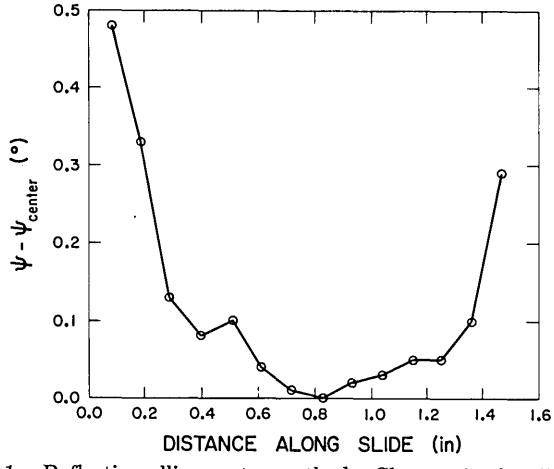

Fig. 1. Reflection ellipsometry method. Changes in the ellipsometric parameter ψ from its value at the center as a function of position on the thick Sc_2O_3 film (λ = 632.8 nm, ϕ = 60°).

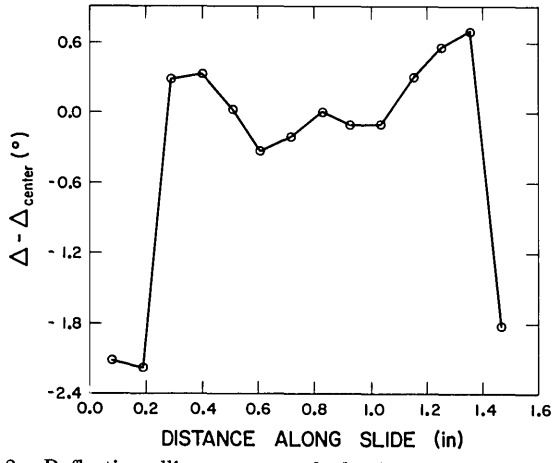

Fig. 2. Reflection ellipsometry method. Changes in the ellipsometric parameter Δ from its value at the center as a function of position on the thick Sc_2O_3 film (λ = 632.8 nm, ϕ = 60°).

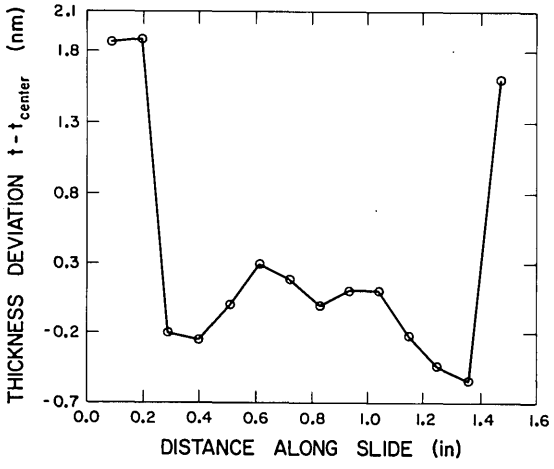

Fig. 3. Reflection ellipsometry method. Changes in film thickness t from its center value as a function of position in the thick Sc_2O_3 film. Obtained from Figs. 1 and 2, assuming a uniform refractive index of 1.81 (λ = 632.8 nm, ϕ = 60°).

For the Sc_2O_3 films, thicknesses t_1 = 228.2 nm and t_2 = 462.6 nm were determined from the λ = 632.8-nm data (t_2/t_1 = 2.03) and were kept constant at other wavelengths.

The refractive index n of Sc_2O_3 obtained by averaging the independently determined indices of the thin and thick films is also shown in Table V. In addition k was computed (k ranged from −0.07 to 0.001), but the results are considered unacceptable.

Table VI gives the thicknesses t_1 and t_2 of the thin and thick Rh films, independently determined at each wavelength by inverting $(\psi,\Delta)_{1-2}$ data on both films at the same angle. The spread with wavelength of t_1 and t_2 of the Rh films is significantly less than that obtained for the Sc_2O_3 films. (The Sc_2O_3 films are shown elsewhere in this paper to be appreciably inhomogeneous.)

The values of n and k of the Rh films obtained (simultaneously with t_1 and t_2) by inversion of the thin- and thick-film data at the same incidence angle are given in Table V. The computed intensity transmittances of the thin and thick Rh films using the optical constants at λ = 546.1 nm are 16 and 5%, respectively. These compare reasonably with 18 and 7% measured transmittances quoted by the OCLI team for $\lambda \simeq$ 550.0 nm. However, n is significantly higher and k lower than corresponding values determined for Rh by Coulter *et al.*[5] 10 years ago.

To test the uniformity of one sample, measurements were made at fourteen equispaced points along a diameter (missing the clear notch area) on the thick Sc_2O_3 film. The He–Ne laser was used at ϕ = 60°, and the illuminated spot size on the sample surface was ~1 mm^2. Figures 1 and 2 show the changes of ψ (psi) and Δ (delta) as a function of position on the Sc_2O_3 film. If a constant refractive index of 1.81 (Table V) is assumed throughout the film, these ψ and Δ profiles lead to the thickness-variation profile of Fig. 3. The film is reasonably uniform, excluding some edge effects.

Null ellipsometry has the advantage of involving only purely angular measurements (no absolute or relative photometry); hence it can be highly accurate. Furthermore, ellipsometry permits the simultaneous determination of film thickness and optical constants from the same data. Its sensitivity to ultrathin films (down to 1 Å) is difficult to match. On the other hand, the ellipsometer is sometimes looked at (unfairly) as a complicated instrument. Certainly, data acquisition needs care, and subsequent inversion is not as simple or straightforward as one wishes. We obviously could not determine the extinction coefficient k of the Sc_2O_3 films using this technique. The estimated accuracy of the ellipsometric determination of n and k is about ±0.1.

C. Wideband Spectrophotometric Method

The technique[16–18] uses normal incidence measurements of R_f and T over a wide spectral range. We applied it to determination of the optical constants of the Sc_2O_3 only. Each layer is assumed to be inhomogeneous with index varying from n_i at the interface with the substrate to n_1 at the interface with air. Then n is the mean index given by $(n_i + n_1)/2$ and $\Delta n = n_1 - n_i$. For calculation, the variation of index between n_i and n_1 is considered to be linear, and the layer is modeled by ten homogeneous sublayers of equal thickness. If j is the order of the sublayer, counted from the substrate, the jth index is given by $n_j = n + \Delta n[(2j - 11)/20]$. In this system of notation, $\Delta n/n$ is negative when the index of the layer decreases from the substrate. Layers that are absorbing are considered to have a constant value of k throughout the set of sublayers.

Both n_j and k are functions of wavelength. Scattering losses are not taken into account separately, and the value obtained for the extinction coefficient simply assumes that all significant losses are due to absorption.

The sample consists of a rectangular substrate coated over half of its area and slightly wedged so that beams reflected from the rear surface are deflected outside the instrumental aperture. It is placed in a goniometer carrying two receivers (silicon photodiodes were used for these measurements), one for R_f and one for T

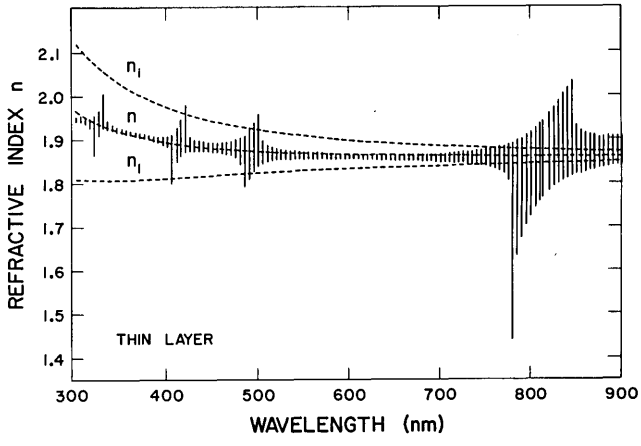

Fig. 4. Wideband spectrophotometric method. Refractive indices n, n_1, and n_i as a function of wavelength for the 447.8-nm thick Sc_2O_3 film. Error bars for n assume that the errors in reflectance and transmittance are 0.003.

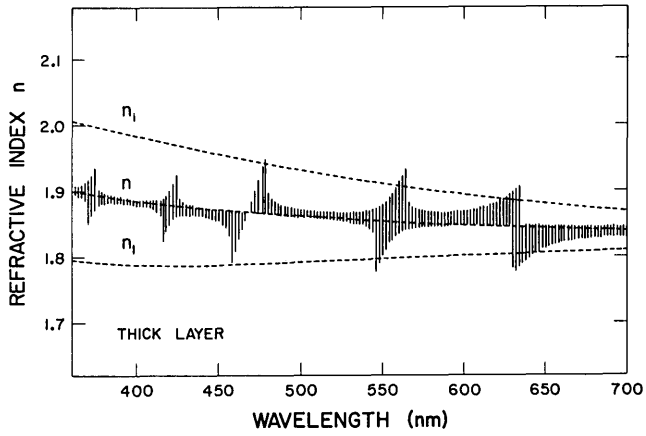

Fig. 5. Wideband spectrophotometric method. Refractive indices n, n_1, and n_i as a function of wavelength for the 217.6-nm thick Sc_2O_3 film.

Table VII. Wideband Spectrophotometric Method: Measured Spectral Reflectance and Transmittance of the Sc_2O_3 Films

λ(nm)	Thin Film		Thick Film	
	R_s	T	R_s	T
300	0.0703	0.9059	0.0699	0.9167
350	0.0449	0.9424	0.1647	0.8312
400	0.0835	0.9077	0.0294	0.9691
450	0.1160	0.8771	0.0707	0.9280
500	0.1372	0.8576	0.1483	0.8507
550	0.0258	0.9709	0.1658	0.8335
600	0.0902	0.9059	0.1446	0.8543
650	0.1531	0.8422	0.1006	0.8985
700	0.1342	0.8614	0.0638	0.9354
750	0.0783	0.9191	0.0403	0.9589
800	0.0392	0.9592	0.0316	0.9678
850	—	—	0.0347	0.9653
900	—	—	0.0452	0.9640

Table VIII. Wideband Spectrophotometric Method: Positions of Reflectance Extrema of Sc_2O_3 Films

t(nm)	λ(nm)	Extremum of R_s	R_s	T
447.8	316	Max	0.170	0.809
	342	Min	0.020	0.967
	379	Max	0.170	0.819
	420	Min	0.020	0.972
	477	Max	0.170	0.823
	554	Min	0.025	0.973
	661	Max	0.155	0.840
217.6	334	Max	0.185	0.813
	412	Min	0.023	0.976
	379	Max	0.167	0.832
	813	Min	0.031	0.968

measurements, and illuminated by a monochromatic beam of light with an angular spread of <2° illuminating an area of 4 × 3 mm of sample. The light is derived from a double-grating spectrometer designed and constructed specifically for this purpose. The monochromator is stepped in wavelength at intervals of 2 nm over the 300–900-nm range, and measurements of signal reflected and transmitted by the coated and uncoated areas of the sample are made at each step, the uncoated measurement acting as a continuous calibration reference since this calculation assumes knowledge of the optical constants of the substrate. With slits of 0.1-mm width the bandwidth of the monochromator is 0.5 nm.

The coated substrates were not cleaned before this particular series of measurements, and the measurements were made in a normal atmosphere.

The fully automatic calculation technique is described in Refs. 16 and 17. The thickness of the film is not required and emerges from the calculation as the sum of the ten equal thicknesses of the sublayers. The refractive index of the substrate must be known accurately as substrate transmittance and reflectance are used as reference values for continuous calibration of the instrument. Values of index n, degree of inhomogeneity $\Delta n/n$, and absorption coefficient k are calculated at 1-nm intervals by a method of successive approximations. At an early stage a value for total film geometrical thickness is derived and is used in the later stages of the computations. It is convenient for subsequent calculations to put n and $\Delta n/n$ in the form of Cauchy expressions such as

$$n = A + \frac{B}{\lambda^2} + \frac{C}{\lambda^4}. \tag{5}$$

The coefficients A, B, and C are automatically produced in a final stage. They were 1.85809, 6.55549×10^4 (Å^{-2}), 7.93018×10^{12} (Å^{-4}) for the thin and 1.8149, 1.24223×10^6 (Å^{-2}), -1.67133×10^{12} (Å^{-4}) for the thick Sc_2O_3 films, respectively.

The calculated values of n, n_i, and n_1 are shown in Figs. 4 and 5. The error bars were based on the assumption that the errors in R_f and T are 0.3%. From the figures it can be seen that the inhomogeneities $\Delta n/n$ at 320 and 900 nm are −13, −2% for the thin and −10, −3% for the thick Sc_2O_3 films, respectively. The absorption coefficient was <0.0006 for both films in the visible part of the spectrum.

It is impossible in a short communication to reproduce all the values of R_s, T as a function of λ, and so selected values only are in Table VII and VIII.

D. Modified Valeev Turning Point Method and the Nestell and Christy Method

Our methods for determining the optical constants and thickness of a thin metal or dielectric film were based on analysis of spectral scans of transmittance and reflectance of the sample. These scans were made on a Cary 17-DX spectrophotometer interfaced to an HP9825T desktop computer for data collection. This spectrophotometer is a dual-beam instrument covering the visible, near UV, and near IR. For this study, we made scans over the 200–900-nm wavelength range using a Hamamatsu R955 photomultiplier tube. The deuterium light source was used for wavelengths shorter than 400 nm, and the tungsten–halogen lamp was used for wavelengths longer than 400 nm. The entire instrument was purged with dry nitrogen, and parts were allowed to equilibrate for at least an hour in the sample compartment prior to taking the spectra.

Transmittance measurements were made by first scanning the transmittance T_w of an uncoated fused silica substrate and then scanning the transmittance T of the coated part to be measured. The transmittance T_{obs} was then calculated as follows:

$$T_{obs} = T/T_w. \tag{6}$$

By using the ratio of these two measurements, the effects of substrate absorption were minimized. The reflection losses for the uncoated substrate and for the coated part were calculated using the dispersion curve for fused silica given in Sec. II. These were taken into account in the analysis.

The reflectance of the dielectric coatings was measured using a specially designed single bounce reflectance attachment. The spectrophotometer light beam was incident on the sample at an angle of 10°, although this deviation from normal incidence was ignored. Only the reflectance from the first surface of the sample was measured. The reflectance of the second surface was eliminated by using an index matching fluid to attach a piece of fused silica to the back of the sample being measured. The second surface of this piece of fused silica was frosted to diffuse the reflected light. The reflectance R_f was determined using

$$R_f = R_{obs}R_{s,c}/R_s, \tag{7}$$

where R_{obs} is the measured reflectance of the coated part, R_s is the measured reflectance of a fused silica witness, and $R_{s,c}$ is the calculated Fresnel reflectance of fused silica.

The reflectance of the metal coatings was measured using the Strong (V-W) reflectance attachment[19] provided with the Cary. This device measures R_f^2 since the light beam reflects twice from the surface of the part. The angle of incidence was 8°, which was assumed to be equivalent to normal incidence. Because the reflectance of the metal coatings was relatively high and the transmittance was low, the effects of the second surface were expected to be small and were ignored.

Each measurement consisted of the appropriate background scan (e.g., with the uncoated part in the beam) followed by the scan of the coated part. This procedure was repeated a number of times for each scan, and the final values represent the average of two or three measurements. In this way, the effects of random fluctuations and drift of the spectrophotometer were minimized.

The dielectric coatings were cleaned with methyl alcohol and a soft towel prior to measurement. The metal coatings were not cleaned. However, care was taken to protect the central portion of the metal coatings where the R_f and T measurements were made.

The thickness and optical properties of the dielectric coatings were determined from scans of T at normal incidence and R_f at near normal incidence. The spectral scans for the thinner Sc_2O_3 sample are shown in Fig. 6. The upper solid curve is T (left scale), and the lower solid curve is R_f (right scale). Each of these curves represents the average of three scans. In addition, the scans have been smoothed using a least-squares fit technique.[20] The dashed curve is the theoretical Fresnel reflectance $R_{s,c}$ of fused silica (right scale). We refer to the following analysis method as a turning point technique, because only the maxima and minima of the scans are used.

Each maximum of the transmittance curve T_{max} corresponds to a halfwave point, i.e., to a wavelength λ where the optical thickness of the coating is an integral number of halfwaves. In terms of the physical thickness t and the average refractive index of the film n, the halfwave points are given by

$$m\lambda/2 = nt, \tag{8}$$

where m is the order number. The value of m is indicated in Fig. 6 for each of the transmittance maxima.

Because the transmittance plotted in Fig. 6 was measured relative to an uncoated part [see Eq. (6)], one would expect the maximum values to be unity. Absorption would result in a maximum T less than one, which occurs for the $m = 4$ peak. The fact that T_{max} is greater than unity in several cases indicates that the film is slightly inhomogeneous. Note that the corresponding

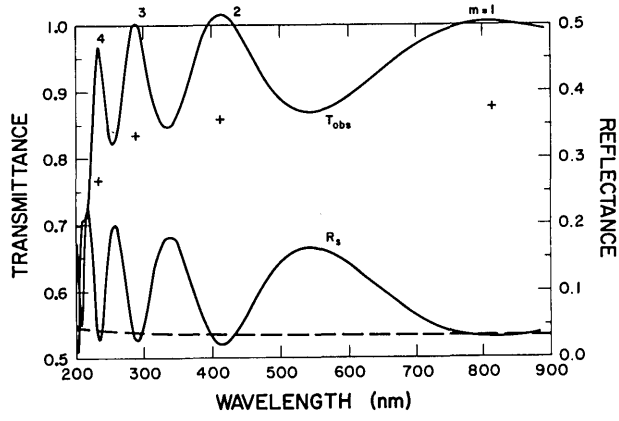

Fig. 6. Modified Valeev turning point method. Measured T_{obs} and R_f for the thinner Sc_2O_3 film (solid curves) and the theoretical $R_{s,c}$ of fused silica (dashed curve). Interpolated minimum values of T_{obs} are indicated by plusses. Order numbers m are given by the corresponding maxima of T.

minimum values of R_f are less than the reflectance $R_{s,c}$ of the uncoated substrate.

The n and k determination was made using the method of Valeev.[21,22] This technique uses the transmittance values at the turning points and gives the optical properties only at the halfwave points. Valeev's method was extended to account for the inhomogeneity. The steps in the analysis were as follows:

(1) The transmittance values at the minima were interpolated to the wavelengths of the maxima. The resulting transmittance values T_{int} are denoted by pluses in Fig. 6.

(2) The average index n and an approximate value of k were determined at the halfwave points from $T_{\max}$, T_{int}, λ, and m using the method of Valeev.[21,22]

(3) A more accurate value of k was determined using

$$k = nA/2\pi m, \tag{9}$$

where the absorption A is given by

$$A = 1 - R_{\min} - T_f. \tag{10}$$

Here $R_{\min}$ is the reflectance [see Eq. (7)] measured at the minimum corresponding to the mth-order maximum of T, and T_f is the maximum transmittance of the coating only—compensating for the effects of the second surface of the substrate. This is given approximately by

$$T_f \cong T_{\max}(1 - R_{s,c}R_{\min})/(1 + R_{s,c}). \tag{11}$$

(4) The degree of inhomogeneity was determined from the reflectance minima using

$$\Delta n \cong n(R_{s,c} - R_{\min})/(4.4R_{s,c}). \tag{12}$$

This is an approximate expression which was arrived at empirically by modeling an inhomogeneous layer by several thin homogeneous ones and making calculations of reflectance for several cases using standard thin-film techniques. In terms of Δn, the index of the film at the substrate interface is given by

$$n_i = n + \Delta n/2 \tag{13a}$$

and at the air interface by

$$n_1 = n - \Delta n/2. \tag{13b}$$

(5) The mechanical or physical thickness t of the film was calculated at each halfwave point using Eq. (8).

The measured and calculated properties of the Sc_2O_3 films are listed in Table IX. The first four lines contain the data for the thinner film, and the next eight are for the thicker film. The last line, labeled ±, indicates our estimate of the accuracy of the data. The wavelength and T and R_f values of the turning points were obtained by fitting the data to a parabola in the neighborhood of each extremum. The order numbers m were assigned to minimize the variation in thickness t.

The average calculated thickness of the thinner film was found to be 219 ± 3 nm. The uncertainty in this value is due to the uncertainty in n. The variation in calculated thickness of the thicker film is somewhat larger, especially at the shorter wavelengths. This is probably due to the dispersive absorption which occurs at these wavelengths and which would tend to shift the calculated values to longer wavelengths. Using the values for wavelengths >290 nm, one finds the average thickness to be 447 ± 5 nm.

Both films possess a significant degree of inhomogeneity for wavelengths shorter than 600 nm. It is peculiar that the films seem to be homogeneous at 800 nm. The calculated inhomogeneity indicates that the index is decreasing toward the air interface. On this basis, one would expect the thicker film to have a lower average index than the thinner sample because the additional material on the thicker film will be of a lower index. From Table IX, this is seen to be the case. To further emphasize this point, the index data are plotted in Fig. 7. The stars represent values of n, and the bars represent the index variation from n_i to n_1. Solid and dashed lines are used to connect the data for the thin and thick samples, respectively. It is clear that n is higher for the thinner sample. Note that the tops of the

Table IX. Modified Valeev Turning Point Method: Data and Results for Sc_2O_3 Films

m	λ (nm)	$T_{\max}$	T_{int}	$R_{\min}$	A	n	Δn	k	t (nm)
4	233.2	0.969	0.767	0.028	0.043	2.14	0.16	0.0037	218
3	287.6	1.003	0.835	0.027	0.008	1.98	0.14	0.0008	218
2	411.6	1.016	0.859	0.022	0	1.90	0.17	0	218
1	813.0	1.004	0.876	0.032	0	1.83	0.03	0	222
9	219.1	0.893	0.733	0.025	0.121	2.11	0.21	0.0045	467
8	235.3	0.953	0.801	0.025	0.062	2.01	0.19	0.0025	468
7	258.7	0.992	0.836	0.020	0.027	1.98	0.23	0.0012	457
6	291.6	1.002	0.853	0.022	0.014	1.93	0.19	0.0007	452
5	341.0	1.015	0.855	0.019	0.004	1.92	0.21	0.0002	444
4	418.6	1.018	0.860	0.019	0	1.89	0.20	0	443
3	552.4	1.012	0.873	0.025	0	1.85	0.12	0	448
2	818.3	0.999	0.877	0.037	0	1.82	0	0	450
±	0.3	0.002	0.002	0.001	0.003	0.01	0.03	0.0002	5

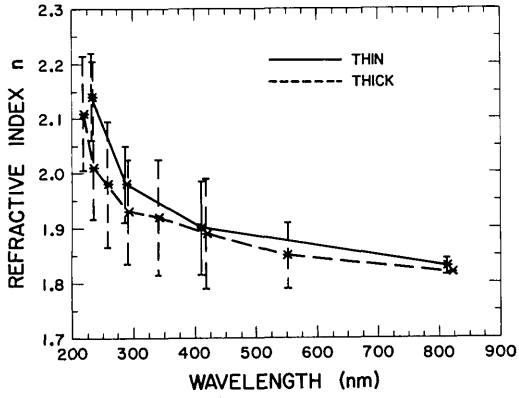

Fig. 7. Modified Valeev turning point method. Measured index and inhomogeneity of the Sc_2O_3 films. Stars indicate average index values. Bars indicate range of index.

bars, representing n_i, are at nearly the same level for both samples, while the bottoms of the bars, representing n_1, are much lower for the thicker sample. This demonstrates that both films have the same index profile.

The advantages of the turning point method of determining optical constants are that (1) it does not require mechanical thickness measurements and (2) it uses the spectral data at the points of greatest sensitivity, accuracy, and simplicity of analysis. Specifically, the index is determined from the minimum value of T (interpolated to T_{int}), which is the most sensitive portion of the transmittance curve to index. The inhomogeneity is determined from R_{min}, where the effects of absorption are negligible. The thickness is determined at the halfway points, whose positions are insensitive to dispersion and inhomogeneity. The determination of the four parameters n, Δn, k, and t are only weakly interdependent on each other in that if they are determined in the proper order, several iterations are not required.

One disadvantage of the turning point method is that data are obtained only at selected wavelengths over a given spectral region. If a sufficient number of data points are obtained, as in Fig. 7, the results can be interpolated to intermediate wavelengths. The minimum thickness for a film analyzed by this technique would be three quarterwaves at a wavelength within the spectral range being scanned. A film this thin would yield data at one point. For best results one would like a film at least seven quarterwaves thick so that several halfwave points can be analyzed. Thus the major shortcoming of the method is that very thin films cannot be analyzed. This is a drawback for thin films which are expected to have radically different properties from thicker ones or in cases where some other factor, such as stress, prevents the growing of a thicker film for analysis. However, in the case of the scandia film analyzed here, the data on inhomogeneity are sufficient to predict the average index of much thinner films.

The thickness and optical properties of the thin metal coatings were determined from scans of T at normal incidence, R_f at near normal incidence, and T for p-polarized light incident on the sample at 60°. These provide three measured values which are sufficiently independent to determine the optical properties n and

Table X. Nestell and Christy Method: Data and Results for Rh Films

λ (nm)	T	$T_p(60)$	R_f	t(nm)	n	k
400	0.168	0.236	0.440	16.4	1.86	2.88
450	0.171	0.245	0.437	16.5	2.04	3.02
500	0.176	0.255	0.432	16.8	2.18	3.14
550	0.178	0.259	0.431	17.8	2.32	3.28
600	0.180	0.264	0.429	17.8	2.46	3.40
650	0.181	0.266	0.428	18.4	2.61	3.52
700	0.181	0.270	0.428	17.2	2.75	3.63
750	0.181	0.271	0.428	18.7	2.88	3.74
800	0.183	0.273	0.427	19.5	2.97	3.86
850	0.184	0.276	0.424	20.0	3.08	3.94
400	0.050	0.069	0.556	30.6	1.86	2.97
450	0.057	0.082	0.560	29.6	1.96	3.12
500	0.062	0.092	0.565	29.7	2.04	3.27
550	0.065	0.099	0.570	29.9	2.13	3.43
600	0.067	0.104	0.575	30.5	2.23	3.59
650	0.069	0.108	0.577	31.0	2.36	3.74
700	0.070	0.111	0.580	31.4	2.47	3.88
750	0.072	0.114	0.581	31.8	2.60	4.01
800	0.073	0.118	0.582	30.9	2.71	4.13
850	0.074	0.121	0.582	32.2	2.81	4.24
±	0.002	0.002	0.002	1.0	0.10	0.05

Note: n and k values were calculated using t = 17.2 nm for the thinner film and t = 30.1 nm for the thicker film.

k and the t of the film. Since the equations for R_f, T, and $T_p(60)$ cannot be solved explicitly for n, k, and t, it is necessary to use an iterative approach to solve for values of n, k, and t consistent with the measured values of R_f, T, and $T_p(60)$. We have used the method of Nestell and Christy.[23]

Spectral data were obtained over the 400–900-nm range at 5-nm intervals. Wavelengths shorter than 400 nm could not be used because the Glan-Thompson polarizing prism used to make the $T_p(60)$ scans was opaque at shorter wavelengths. The data represent the average of two scans. Data at 50-nm intervals for T, $T_p(60)$, and R_f are listed in Table X. The upper set of data refers to the thinner film, and the lower set refers to the thicker film. The row of values at the bottom labeled ± contains our estimate of the accuracy of the data.

The method of Nestell and Christy involves three steps:

(1) Solve for n, k, and t consistent with T, $T_p(60)$, and R_f at each wavelength. Because the calculations at each wavelength are independent of each other, the calculated value of t may not be (in fact, is usually not) the same at all wavelengths. This is probably due to inhomogeneities in the film expected to be present in very thin metal films. Table X lists the values of t in nanometers calculated from the spectral data. They tend to increase at longer wavelengths. This behavior may be due to a slight oxidation of the outer surface of the film[24] or from effects of nucleation.

(2) A best average value of the thickness of the film is determined from the values obtained in the short-wavelength region of the visible spectrum. Over this spectral range, the uncertainty in the value of t is the smallest, and the variation due to oxidation effects is also minimal. Values of 17.2 ± 1.2 and 30.1 ± 1.2 nm were obtained for the thicknesses of the thin and thicker films, respectively. These values were found by averaging t over the 400–650-nm range. The uncertainty in thickness of the thinner film is due to the variation in calculated values of t, while the uncertainty in the value for the thicker film results from our estimate of the accuracy of the spectral measurements. Note that the thicker film is slightly less than twice as thick as the thinner film.

(3) Using the thickness calculated in step (2), all the data were reanalyzed using only the scan of T and R_f to give self-consistent values of n and k. [Thus note that the value of $T_p(60)$ was used only in determination of the thickness.] The resulting values calculated for n and k for the two films are listed in the last two columns of Table X.

A graph of the n and k data for the two films is plotted in Fig. 8 together with Hass's previous data for Rh[5] which are indicated by crosses. The solid and dashed curves refer to the thin and thick Rh films, respectively. The lower two curves and lower set of Hass's data are the values for n (left scale). The upper two curves and upper set of Hass's data are the k values (right scale). From Fig. 8, it is apparent that the present results are not in close agreement with Hass's earlier measurements. This may be due in part to the fact that Hass measured a thicker film. However, the difference may be due to actual differences in film properties resulting from different film preparation techniques.

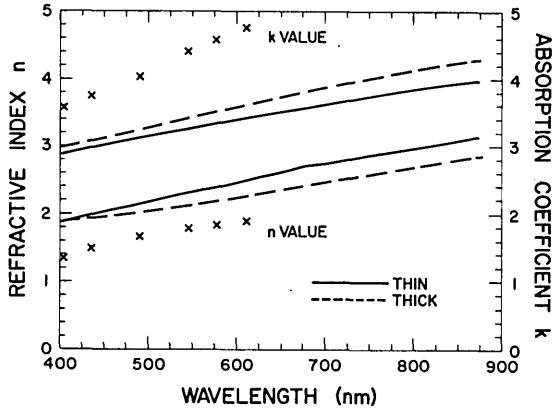

Fig. 8. Nestell and Christy method. Measured n and k for the Rh films. Crosses represent Hass's data.[16]

A major difficulty with the Nestell-Christy method is obtaining spectral data with enough accuracy. The method is especially sensitive to small errors in T. In particular, errors in the measurement of T and $T_p(60)$ result in a significant uncertainty in the calculated value of t, which then becomes the limiting factor in the determination of n and k. As indicated in Table X, an uncertainty of ±0.002 (0.2%) in the value of T results in an error of 1.2 nm in the value of t. These errors are relatively larger for thicker films, which have much lower transmittances. Thus the method is most useful for metal films with T in the range from 0.03 to 0.3 or so.

A second and potentially more serious drawback of the method is that the solution for n, k, and t is not unique, and incorrect solutions (or no solution) may be obtained if incorrect starting values are chosen. Having two similar films of different thicknesses is a distinct advantage here—especially if the ratio of the thicknesses is known, because the possibility of achieving similar spurious solutions for both films is very small.

A major advantage of the method is that only spectral data are required, and, in particular, the physical thickness need not be measured directly. With careful measurement techniques and a satisfactory computer code for data analysis, n and k data sufficiently accurate for optical coating design and analysis can be obtained.

E. Algebraic Inversion Method

A new analytical method[25] provides the basis for deriving optical constants presented in this paper. Although algebraic in content, the method permits location of the unknown film anywhere within a complex multilayer. It takes reflectance and transmittance (at a single wavelength, angle of incidence, and polarization) as input and returns all combinations of refractive index, absorption coefficient, and thickness that are

Table XI. Algebraic Inversion Method: Spectrophotometric Data and Refractive-Index Solutions for Sc_2O_3 Films

λ (nm)	t = 225 ± 5 nm		t = 450 ± 10 nm	
	T	n	T	n
400	0.9341	(a)	0.8804	(a)
450	0.9020	1.84 ± 0.04	0.8590	1.87 ± 0.02
500	0.8283	(b)	0.8318	1.86 ± 0.02
550	0.8093	1.87 ± 0.03	0.9415	(a)
600	0.8321	1.84 ± 0.02	0.8874	1.87 ± 0.02
650	0.8703	1.82 ± 0.02	0.8251	1.82 ± 0.03
700	0.9045	1.81 ± 0.04	0.8383	1.83 ± 0.02

(a) No solution for measured T and film thickness; solution at 220 nm thickness is n = 1.89 ± 0.09.

(b) No solution in the 1.8 to 1.9 index range for a homogeneous film.

Within measurement accuracy, R + T = 1, and k = 0.

Δn based on ΔT = ± 1% and measured film thickness; Δn based on thickness error would be about 3 × as large.

Table XII. Algebraic Inversion Method: Spectrophotometric Data and Optical Constants for Rh Films

λ (nm)	R	R'	T	t = 12 nm		t = 14 nm		R	R'	T	t = 27.5 nm	
				n	k	n	k				n	k
400	0.4469	0.2335	0.1540	2.50	3.45	2.20	3.20	0.5465	0.3493	0.0460	2.40	3.00
450	0.4412	0.2252	0.1571	2.75	3.55	2.45	3.30	0.5485	0.3450	0.0520	2.75	3.15
500	0.4317	0.2151	0.1616	3.10	3.55	2.70	3.45	0.5505	0.3371	0.0569	3.00	3.15
550	0.4314	0.2160	0.1633	3.20	3.75	2.85	3.55	0.5551	0.3438	0.0598	3.10	3.30
600	0.4305	0.2148	0.1650	3.30	3.90	2.95	3.70	0.5608	0.3454	0.0621	3.30	3.40
650	0.4303	0.2147	0.1662	3.35	4.15	3.00	3.85	0.5636	0.3494	0.0640	3.35	3.50
700	0.4288	0.2143	0.1673	3.60	4.20	3.10	3.95	0.5658	0.3511	0.0656	3.50	3.60

These results are based on transmittance and reflectance measured from the film side of both samples.

Table XIII. Algebraic Inversion Method: Refractive Index of SiO_2

λ (nm)	T	n_s(a)	n_s(b)
400	0.9281	1.479	1.470
450	0.9302	1.470	1.466
500	0.9337	1.454	1.462
550	0.9322	1.461	1.460
600	0.9335	1.455	1.458
650	0.9363	1.443	1.457
700	0.9335	1.455	1.455

(a) Refractive indices derived from Vought transmittance data.

(b) Refractive indices calculated from dispersion equation given in Ref. 14.

consistent with the input data. In the present case, independent measurements of film thicknesses were used to narrow the range of solutions.

Transmission and reflectance were measured with a Perkin-Elmer model 330 spectrophotometer and the data recorded on a Perkin-Elmer model 3600 data station. In our laboratory, the double-beam mode is employed routinely, ambient air from a clean room environment (50% relative humidity) filling the instrument. For reflectance, two plane mirrors are inserted, the first deflecting the incident beam onto the sample at an angle of ~10° from normal and the second turning the reflected beam back down the instrument optical axis. Transmittance data are normalized to the transmission of an empty sample holder; reflectance data are normalized with respect to aged vacuum-deposited aluminum on glass (NBS Standard Reference Material 2003a). We estimate the accuracy of the transmittance and reflectance measurements at ±1.0%.

The samples were cleaned prior to measurement by pulling a tissue wetted with a few drops of ethanol across the horizontal sample surfaces until no liquid remained. This technique scratched the thick Rh film surface noticeably, so the thin Rh film was measured without cleaning.

Spectrophotometric data are presented at selected visible wavelengths for all film samples in Tables XI and XII. Reflectance was measured twice, once with the instrument beam incident onto the film surface R and again with the beam incident onto the back surface of the substrate R'.

Thicknesses were measured for the Sc_2O_3 samples using a stylus profilometer (Tencor Alpha-Step profilometer) with a precision of ±10 nm, established by scanning a standard supplied by the manufacturer. The step on each sample was scanned in several locations, and these values differed at most by ±5 nm. Overall, we estimate the thicknesses of the Sc_2O_3 films to be 225 ± 5 and 450 ± 10 nm. For the Rh films, thicknesses were determined by the Tolansky[26] method using a Sloan model M-100 angstrometer. Several fringe patterns for each sample were photographed and measured. These thickness results are 12 ± 2 and 27.5 ± 4.5 nm.

We call attention to a few simplifying assumptions in connection with the data analysis. A polarizer was not available for the photometric measurements, so normal incidence of light was assumed in all computations. We did not find that this approximation introduced errors comparable with the instrumental precision of the spectrophotometer. Also the sum of reflectance and transmittance measured for each Sc_2O_3 film was within these same instrumental limits. Therefore we assumed the Sc_2O_3 material to be nonabsorbing with negligible surface scattering. Finally, for both materials, we used as a model for computing optical constants a homogeneous film with planar parallel surfaces.

The refractive index of the bare substrate material (fused silica) was derived from transmission measurements at a number of wavelength points in the visible spectrum. These values are in excellent agreement with

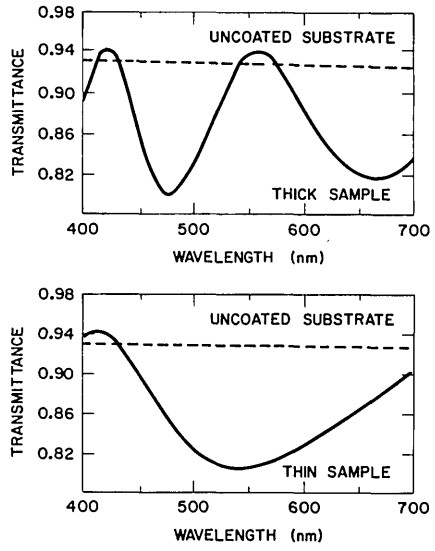

Fig. 9. Algebraic inversion method. Comparison of transmittance T between the Sc_2O_3 samples and the uncoated substrate. Note the intersections near the 420- and 560-nm wavelength.

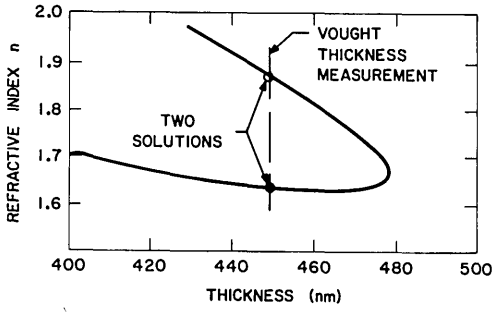

Fig. 10. Algebraic inversion method. Example of data reduction. Two index solutions exist at the measured film thickness. However, the solution between n = 1.8 and 1.9 is believed to be the correct choice.

earlier work,[14] as shown in Table XIII. Measured transmittances for the two Sc_2O_3 samples are presented in Fig. 9, and each is compared with similar data for the uncoated substrate. The intersections of these curves present a problem in analysis as discussed below. Figure 10 shows one example of computer-generated output derived from input transmittance data for the thick Sc_2O_3 film. The trace of solution points defines a locus of index and thickness values consistent with measured transmittance at 600-nm wavelength. Two of these solution points are compatible with our 450-nm thickness measurement. In general such solution traces exist in separate optical thickness ranges according to

$$\frac{(m-1)\lambda}{2} \le nt < \frac{m\lambda}{2}, \qquad m = 1,2,\ldots, \tag{14}$$

and only the m = 3 output is shown in Fig. 10.

Given the multiplicity of solutions at each wavelength, additional measurements are desirable, say transmittance at large angles of incidence. Nevertheless, only index values between 1.8 and 1.9 emerge as consistent with both Sc_2O_3 films. All other solution paths were highly dispersive.

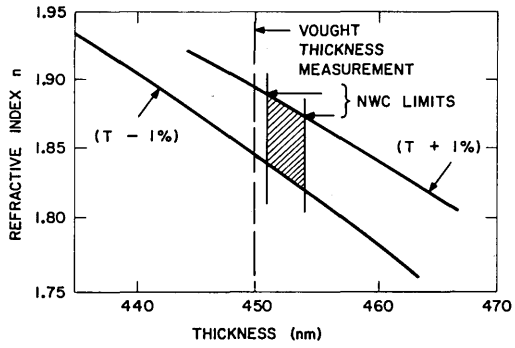

Fig. 11. Algebraic inversion method. Example of error analysis (NWC = Naval Weapons Center, China Lake, Calif.).

In certain spectral regions, near 420- and 500-nm wavelength, the transmittance of a film sample exceeds that of the uncoated substrate (see Fig. 9). At these wavelengths, it is not possible to model the film as homogeneous material with refractive index greater than that of the substrate. Here our computer program correctly outputs lower index solutions. We conclude that the Sc_2O_3 films are somewhat inhomogeneous.

Sensitivity to measurement errors, and hence the precision in our results, was determined by examining the solution traces for inputs incrementally above and below our actual measurements. An example of error analysis is shown in Fig. 11. Corresponding to our confidence limits in sample thickness t and transmittance T, respective sensitivities of the index n with respect to these measurement parameters are related by

$$\left(\frac{\partial n}{\partial t}\right)\Delta t \sim 3\left(\frac{\partial n}{\partial T}\right)\Delta T. \tag{15}$$

However, with the greater precision quoted for a similar sample by personnel at the Naval Weapons Center, the relationship is

$$\left(\frac{\partial n}{\partial t}\right)\Delta t \sim \tfrac{1}{2}\left(\frac{\partial n}{\partial T}\right)\Delta T. \tag{16}$$

Results of our analysis for the Sc_2O_3 films are summarized in Table XI.

The algebraic method for extracting optical constants is suitable also for absorbing films. An example of solution traces is shown for the thick Rh film in Fig. 12. Since the film absorbs, both reflectance and transmittance data were needed in the computer program to determine n and k. The solution traces depicted in Fig. 12 were generated using reflectance measured from the film side of the sample. All traces for the thick sample had a general S shape giving rise to three potential solutions in the vicinity of the measured thickness, 27.5 nm. However, only the low n and corresponding high k parts of the S curves (labeled 1 in Fig. 12) were consistent with both the thick and thin samples. These optical constants are listed in Table XII. Results are given for two different assumed thicknesses of the thin sample, emphasizing the option of thickness as a parameter rather than a required measurement quantity. In this case, increased values of the thickness parameter correspond to reduced values of k (see Fig. 12)—a trend consistent with the collective results listed in Table XVIII.

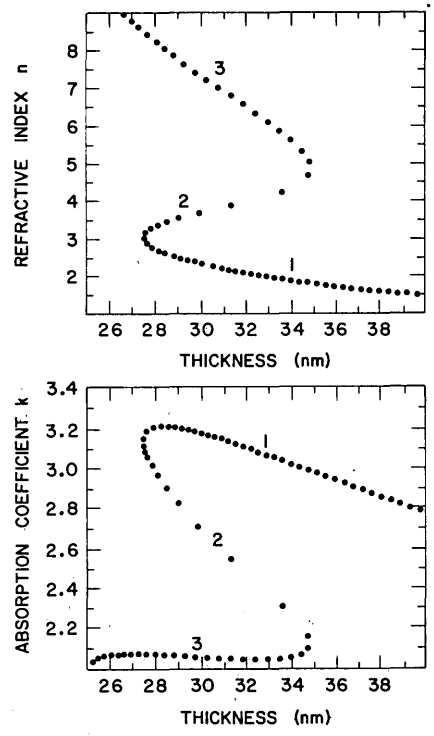

Fig. 12. Algebraic inversion method. Solution traces for the thick Rh film at 500-nm wavelength. Corresponding parts of the n and k curves are labeled 1, 2, and 3.

Repeating the analysis with reflectance data measured from the substrate side only yielded n and k solutions in agreement with those in Table XII for film thicknesses significantly outside previously stated error margins. We conclude that the Rh material is also inhomogeneous.

Finding multiple solutions for n and k at the same film thickness is a direct consequence of inverting nonlinear optical equations. To resolve the ambiguity, we recommend additional measurements at different angles of incidence and polarization. Another possibility is to select those optical constants consistent with two or more thicknesses of the same material—the procedure followed in this paper.

In summary, we have applied a new algebraic method to extract thin-film optical parameters from spectrophotometric data. The method permits a determination of all n, k, and film thickness combinations at a single wavelength compatible with measured reflectance and transmittance. These solution points lie along continuous curves, easily mapped to any level of detail for purposes of exactness and error analysis. We believe that gaining this perspective on the total solution space is highly advantageous.

F. Inverse Synthesis Method

This method is described at some length in Ref. 27. It is a multiwavelength multiangle method in which the constants of suitable dispersion formulas are found by numerical refinement that simultaneously best fit many experimental measurements of transmittance, reflectance, and/or absorptance. The dispersion equations we employed for the current determinations were

$$n^2 = A + k^2 + \frac{B\lambda^2}{(1 + C^2\lambda^2)} + \sum_{i=1}^{2}\left[\frac{B_i\lambda^2(\lambda^2 - C_i^2)}{(\lambda^2 - C_i^2)^2 + D_i^2\lambda^2}\right]$$

$$k = \frac{1}{2n}\left\{\frac{BC\lambda^3}{(1 + C^2\lambda^2)} + \sum_{i=1}^{2}\left[\frac{B_iD_i\lambda^3}{(\lambda^2 - C_i^2)^2 + D_i^2\lambda^2}\right]\right\}, \quad (17)$$

where λ is expressed in microns, and A,B,C,B_i,C_i,D_i are suitable constants. Many different thin-film models are possible. For the purpose of this determination we assumed that all films are homogeneous, absorbing, but scatter-free and that the optical constants for both the thin and thick films are the same.

The samples were not cleaned prior to the measurements, and ambient atmospheric conditions and temperatures prevailed. The thicknesses of the metal films were measured with a Sloan Dektak II profilometer. A Perkin-Elmer model 330 spectrophotometer was used for the spectral transmission and reflection measurements. For the latter a reflectance attachment was employed. Measurements on the uncoated substrates were consistent with the published optical constants for silica.[3] For transmission measurements at non-normal incidence, polarizers were placed in both beams of the instrument, and the spectrophotometer was zeroed prior to insertion of the sample.

For determination of the optical constants of Sc_2O_3 we measured spectral transmission and reflection of each film at normal incidence and the transmission for light polarized parallel and perpendicular to the plane of incidence for angles of 45 and 60° [Figs. 13(A),(B)].

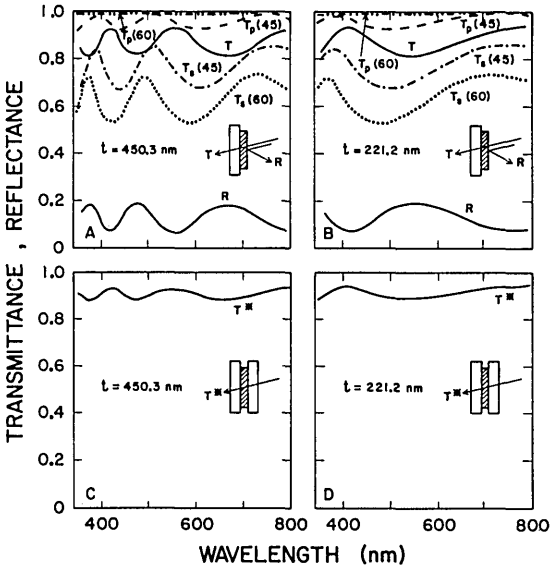

Fig. 13. Inverse synthesis method. Spectrophotometric measurements used in determination of the optical constants of the Sc_2O_3 films.

We also measured the normal incidence transmittance of the films after a quartz plate was contacted to each with a refractive-index matched liquid [Figs. 13(C),(D)]. We assumed that the optical constants of the films immersed in the contact liquid would be unchanged.

We thus obtained fourteen spectral transmittance and reflectance curves for effectively four different thin-film systems. From these curves we selected 196 equispaced points. (This is too large a number to present in tabular form in this paper.) Our computer program tried to fit all these data simultaneously by

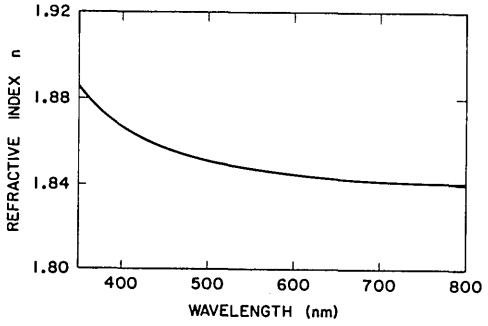

Fig. 14. Inverse synthesis method. Average refractive index of the Sc_2O_3 films.

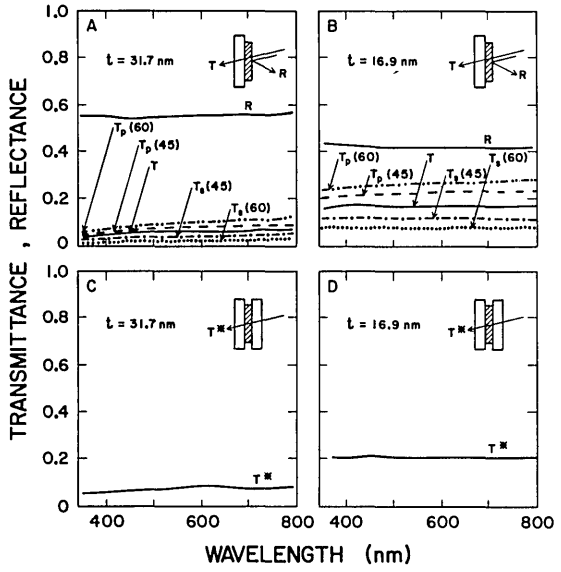

Fig. 15. Inverse synthesis method. Spectrophotometric measurements used in determination of the Rh films.

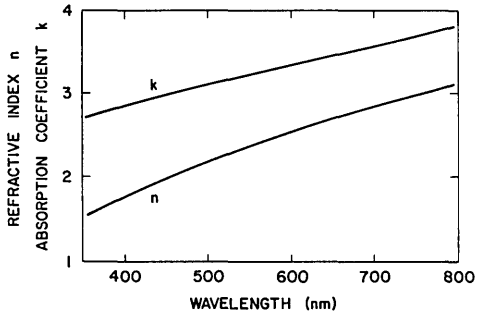

Fig. 16. Inverse synthesis method. Average optical constants of the Rh films.

varying the two thicknesses of the films and the constants of one set of dispersion equations. When the best fit was obtained, the departure between the calculated and experimentally measured points was 1.1%. This corresponds roughly to the accuracy of our spectrophotometric measurements. The dispersion equation constants A,B_1,C_1,D_1 were 3.15, 0.212, 0.244, and 0.000287, respectively. B,C,B_2,C_2, and D_2 were zero. The resulting refractive index of Sc_2O_3 is shown in Fig. 14. In the same spectral region the calculated absorption coefficient was $<2 \times 10^{-4}$. We concluded that, within our experimental accuracy, the Sc_2O_3 films are nonabsorbing.

We used the same type of measurement for determination of the optical constants of Rh (Fig. 15). However, because the films are too thin to show marked fluctuations in the transmittance or reflectance due to interference effects in the spectral region examined, an independent measurement of the thicknesses of the films was essential. We selected 88 points from the curves of Fig. 15 for the calculations. After refinement of the constants of the dispersion equations, the average departure between the experimental and calculated points was 0.8%. The results of our determination of the optical constants of the Rh films are shown in Fig. 16. The values of the dispersion equation constants $A,B,C,B_1,C_1,D_1,B_2,C_2,D_2$ were 162.0, 5.57, −8.92, 208.0, 6.58, 95.9, 20.1, −110.0, and 23.6, respectively.

We feel that the method of inverse synthesis has several advantages. It is equally applicable to absorbing and nonabsorbing materials. With it we can vary the complexity of the thin-film model almost at will. (For example, we could have assumed that the layers are inhomogeneous.) The computer calculations with this method do not cost much.

Because a larger number of measurement points are fitted, nonsystematic errors are averaged out. With this method it is hard to estimate the absolute accuracy of the determination. Still, we feel that even though the present determination was based on measurements taken on a convenient to use, but not very accurate, commercial spectrophotometer, the optical constants obtained are quite adequate for the design and construction of many types of reasonably complicated optical multilayer systems. Clearly the measurements were not adequate for determination of small absorption coefficients such as those of Sc_2O_3 in the visible part of the spectrum. But given more precise measurements, the inverse synthesis method should yield much better results even for this case.

G. Bennett and Booty Method

An iterative search technique similar to that described by Bennett and Booty[28] was used to determine the optical constants of the thin Rh film. In this method measurements at 8° off normal incidence of the front surface reflectance, the normal transmittance and physical thickness of the film are used in an iterative search of possible n,k values. The transmittance and reflectance are calculated using the matrix method

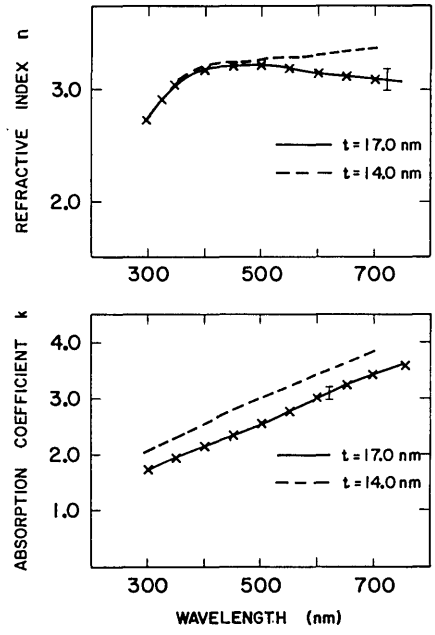

Fig. 17. Bennett and Booty method. Optical constants of Rh. The broken curve represents the results based on the thickness supplied by the Michelson Laboratory (Sec. III.A).

described by Born and Wolf,[29] including coherent reflections in the film and incoherent reflections in the substrate. The calculation uses the approximation that the reflectance at 0 and 8° incidence is the same. The differences $(R - R_c)^2$ and $(T - T_c)^2$ are minimized in an univariate search; the back reflectance R' is used as a check on the results.

The film was assumed to be homogeneous, and uniform in thickness and optical properties over a fairly large area, as a double-bounce measurement of the reflectance is used. Scattering was not included in the description, and the substrate was assumed to be nonabsorbing and to have a refractive index of 1.460.

The thickness of the film was measured with a Tencor Alpha-Step stylus profilometer. The average value of six passes was used in the calculation of n and k.

The spectral measurements were made on a Cary 14 spectrophotometer. The samples were measured in air without cleaning other than compressed gas removal of surface dust. Transmittance was measured in a single pass; the reflectance was measured using a V-W attachment and by taking two bounces off the sample. Table XIV shows the input data (R, R', and T) and results of the calculation (R_c,R'_c,T_c,n,k).

The values of thicknesses measured at the Michelson Laboratory (Sec. III.A) were used in a comparative calculation to test the sensitivity of the routine to the input thickness, even though these thicknesses were outside the estimated error in our measurement. Results are shown in Fig. 17.

The technique is most sensitive to errors in the front surface reflectance and least sensitive to errors in the thickness determination. Errors in the transmittance and changes in the initial search parameters also lead to differences in the iteratively determined values of n

Table XIV. Bennett and Booty Method: Data for Thin Rh Film

λ (nm)	n	k	R	R_c	T	T_c	R'	R'_c
350.	3.00	1.92	0.4225	0.4225	0.1625	0.1624	0.2842	0.2839
400.	3.16	2.15	0.4342	0.4341	0.1540	0.1565	0.2906	0.2906
450.	3.19	2.34	0.4292	0.4296	0.1575	0.1599	0.2817	0.2809
500.	3.22	2.54	0.4274	0.4276	0.1622	0.1611	0.2767	0.2751
550.	3.19	2.79	0.4254	0.4259	0.1638	0.1614	0.2742	0.2702
600.	3.15	3.03	0.4249	0.4247	0.1646	0.1627	0.2724	0.2669
650.	3.13	3.26	0.4258	0.4262	0.1656	0.1631	0.2730	0.2675
700.	3.07	3.47	0.4250	0.4247	0.1660	0.1667	0.2717	0.2656
750.	3.07	3.61	0.4219	0.4217	0.1672	0.1771	0.2696	0.2622

Table XV. Bennett and Booty Method: Effect of Perturbations on Optical Constants Determination

Artificial Error	% Change in n, k
1% added to R	1.0-6.0% (worse at long wavelength)
1% added to T	0.5-4.0% (worse at long wavelength)
different search initiation	1.0-2.0% (worse at long wavelength)
6% change in thickness	5.0-6.0% (worse at long wavelength)

and k. Sensitivities were investigated by introducing artificial errors in the data. The results are summarized in Table XV.

The calculated reflectance and transmittance values agree, as shown in Table XIV, to within 0.1 and 1.7%, respectively. The back surface reflectances, which are used to check for incorrect solutions, agree to within 2%. The great sensitivity to R occurs because these data take precedence in the iterative calculation; the transmittance data could be given greater weight if desired.

The advantage of this technique is that it provides n,k information over a wide spectral range very quickly. It works best when n and k have dissimilar values, and the program used here was optimized for the case where n and k differ by a factor of ~10. As in all iterative search procedures, there is a danger of selecting an incorrect (n,k) pair; this problem is worst when n and k have weak spectral variation and similar values. The technique is quite sensitive to measurement errors and to the initializing values of n and k for the search. It also requires that the film be uniform over a lateral distance of ~5 cm (~2 in.).

H. Envelope Method

Our original intention was to use the method of Manifacier *et al*,[30] which requires measurements of normal incidence transmittance only, to determine the optical constants of the Sc_2O_3 films. In this method the layer is assumed to be homogeneous and absorbing. Envelopes are drawn through the maxima and minima of the transmittance curve, and the calculation proceeds on the assumption that these envelopes correspond to the transmittance of integral halfwave and quarterwave thicknesses. Unambiguous determination of n, k, and t is possible. The method is useful for layers that have only slight absorption but breaks down in the presence of heavy absorption. The transmittance traces revealed the presence of considerable inhomogeneity, however, and so the method could not be used. The idea of envelopes was retained, but an inhomogeneous model was adopted for the layer, and measures were made of both R and T. The maxima and minima of R and T were then determined and assumed to correspond to quarterwaves and halfwaves. The remainder of the envelopes was found by linear interpolation or, where necessary, by extrapolation.

A nonabsorbing inhomogeneous layer, provided it is reasonably thick and there is appreciable index contrast at its boundaries, can be represented by the characteristic matrix:

$$\begin{bmatrix} (n_i/n_1)^{1/2}\cos\delta & i(\sin\delta)/(n_1 n_i)^{1/2} \\ i(n_1 n_i)^{1/2}\sin\delta & (n_1/n_i)^{1/2}\cos\delta \end{bmatrix}, \tag{18}$$

where n_1 is the index at the outer interface of the film, n_i at the inner, and δ is the phase thickness of the layer. We assume that the absorption is very small and that in such a case the layer can be represented by an expression of the form (18) with the absorption coefficient included in δ only so that

$$\delta = 2\pi(n - ik)t/\lambda = \alpha + i\beta, \tag{19}$$

where n is the mean index of the film, i.e.,

$$n = (1/d)\int_0^t n(z)dz = 0.5(n_1 + n_1).$$

Here β is assumed to be sufficiently small for first-order expansions in β to be of acceptable accuracy.

We assume in the calculations that the quarterwaves and halfwaves are given by $\alpha = m\pi/2$. We also assume that the same value of β applies to both halfwaves and quarterwaves at the same wavelength. We write $T_{\min}$, $R_{\max}$, $T_{\max}$, and $R_{\min}$ for the transmittance and reflectance corresponding to quarterwave and halfwave thicknesses, respectively. If

$$\begin{aligned} x &= n_o n_s/(n_1 n_i)^{1/2} + (n_1 n_i)^{1/2}, \\ y &= n_o n_s/(n_1 n_i)^{1/2} - (n_1 n_i)^{1/2}, \\ p &= n_o (n_i/n_1)^{1/2} + n_s (n_1/n_i)^{1/2}, \\ q &= n_o (n_i/n_1)^{1/2} - n_x (n_1/n_i)^{1/2}, \end{aligned} \tag{20}$$

then, neglecting terms of second and higher order in β,

$$\begin{aligned} (x + \beta p)^2 &= 4 n_o n_s / T_{\min}, \\ (p + \beta x)^2 &= 4 n_o n_s / T_{\max}, \\ (y + \beta q)^2 &= 4 n_o n_s (R_{\max}/T_{\min}), \\ (a + \beta y)^2 &= 4 n_o n_s (R_{\min}/T_{\max}). \end{aligned} \tag{21}$$

In the present case, y and q are negative, and so we take negative roots for R and positive for T. The iterative scheme for the calculation of n_1, n_i, and β is then

$$\begin{aligned} x &= 2(n_o n_s/T_{\min})^{1/2} - \beta' p', \\ p &= 2(n_o n_s/T_{\max})^{1/2} - \beta' x', \\ y &= -2(n_o n_s R_{\max}/T_{\min})^{1/2} - \beta' q', \\ q &= -2(n_o n_s R_{\min}/T_{\max})^{1/2} - \beta' y', \end{aligned} \tag{22}$$

$$\beta = \frac{0.5C[(1 - T_{\min} - R_{\max})/T_{\min}] + [(1 - T_{\max} - R_{\min})/T_{\max}]}{[(n_s/n_i + n_i/n_s) + \beta']},$$

where β', p', etc. are the values obtained in the previous iteration. Then

$$\begin{aligned} n_1 &= n_o \left[\frac{(x - y)(p - q)}{(x + y)(p + q)}\right]^{1/2}, \\ n_i &= n_s \left[\frac{(x - y)(p + q)}{(x + y)(p - q)}\right]^{1/2}. \end{aligned} \tag{23}$$

If we assume that the optical thickness is given by $(n_1 + n_i)t/2$, we can derive the geometrical thickness from the wavelengths corresponding to the extrema. The values measured from the transmittance curves are assumed for these, since the positions of the reflectance extrema may be slightly displaced by the small angle of incidence. The necessary expression is

$$2\pi[(n_1 + n_i)/2](t/\lambda) = m\pi/2. \tag{24}$$

The order m, an integer, can readily be established from the range of extrema, and then a value of t can be found from each extremum. The final value of t is calculated as the mean of the individual values. Next k is given by

$$k = \delta\lambda/(2\pi t). \tag{25}$$

The derivations so far have used the single-surface reflectance and transmittance. The quantities that are actually measured include the effect of the rear surface and must be corrected. Also the index of the substrate n_s must be known.

Incoherent multiple-beam summation that assumes absorption is confined to the surface coatings yields for the net transmittance T and reflectance R:

$$T = \frac{T_s T_f}{(1 - R_s R_f)} \qquad R = \frac{R_f - R_s(R_f^2 - T_f^2)}{(1 - R_s R_f)}, \tag{26}$$

where T_s, R_s and T_f, R_f are the reflectances and transmittances of the two surfaces. If T_f, R_f refer to the coated surfaces in this case,

$$T_f = \frac{T(1 - R_s R_f)}{T_s} \qquad R_f = R(1 - R_s R_f) + R_s(R_f^2 - T_f^2), \tag{27}$$

and these two expressions can be used in an iterative solution for T_f and R_f given T and R, the measured values, and T_s and R_s the values corresponding to the rear uncoated substrate surface. T_s and R_s can be found from a separate measurement on an uncoated substrate. In this case we assume no absorption either at the interface or through the bulk and obtain

$$T_f = T_s \qquad R_f = R_s = 1 - T_s, \tag{28}$$

so that

$$T_s = 2T/(1 + T) \qquad R_s = (1 - T)/(1 + T). \tag{29}$$

Finally, n_s can then be found from R_s as

$$n_s = \frac{(1 + R_s^{1/2})}{(1 - R_s^{1/2})}. \tag{30}$$

Measurements were made over the 300–700-nm range on a Cary 14 spectrometer. A V-W absolute reflectance attachment was used for the reflectance measurements. Transmittance measurements were made at normal incidence but reflectance at 8°. The V-W attachment gives R^2 and uses two small neighboring areas of the sample so that errors in uniformity may lead to reflectance errors. Both coated and uncoated substrates were measured together with background and zero scans.

Although it is possible to obtain values over the entire wavelength region, the derivations in this example have been limited to the wavelengths corresponding to the extrema. Table XVI shows the reflectance values corrected for the effects of the rear surface together with the value derived for n_s. The values of wavelength correspond to the extrema of the transmittance curves, although there is little difference, if any, between the positions of the extrema in R and T. The values of n_s are quoted to four decimal places not as an indication of possible accuracy but because they are used in subsequent calculations.

Table XVI also shows the derived values of n_1, n_i, k, and t. Note that k is negative for the final two wavelengths corresponding to the thick film. This is simply because the values of R and T sum to slightly greater than unity. Within the accuracy of the measurement (see below) we can simply say that k is virtually zero.

The consistency of the measurement is illustrated by the results in the last column of Table XVI, which are

Table XVI. Envelope Method: Data and Results for Sc_2O_3 Films

λ(nm)	R_{max}	T_{min}	R_{min}	T_{max}	n_s	n_1	n_i	k(x10³)	t(nm)	R + T
333	0.1816	0.8079	—	—	1.4967	1.830	2.038	0.950	215.2	0.9944
415	—	—	0.0219	0.9746	1.4705	1.809	1.980	1.064	219.1	0.9994
551	0.1610	0.8321	—	—	1.4497	1.775	1.914	1.153	224.0	1.0000
315	0.1758	0.8150	—	—	1.4925	1.810	2.021	0.491	452.2	0.9972
344	—	—	0.0205	0.9731	1.4754	1.804	1.999	0.414	452.3	0.9989
377	0.1742	0.8230	—	—	1.4751	1.796	2.000	0.302	446.8	0.9998
421	—	—	0.0186	0.9763	1.4665	1.787	1.993	0.273	445.5	1.0006
478	0.1719	0.8272	—	—	1.4587	1.802	1.957	0.150	445.1	1.0009
555	—	—	0.0255	0.9754	1.4453	1.810	1.895	-0.616	449.4	1.0023
668	0.1569	0.8451	—	—	1.4538	1.819	1.847	-0.496	455.7	0.9992

The mean thicknesses of the thin and thick films are 219.4, 449.6 nm respectively.

the sum of R_s and T_s measured for the uncoated substrate and uncorrected for the effect of the second surface. It suggests that a figure of ±0.002 absolute might be used for the error in R and T in precision calculations. Recalculation of the film parameters using values perturbed by this amount indicates a precision of just under ±0.02 absolute in index, $\pm 2 \times 10^{-3}$ in β, which is a precision in k varying from $\pm 2.5 \times 10^{-4}$ at the short wavelength end to $\pm 5 \times 10^{-4}$ at the long-wavelength end and ±0.5 nm in thickness for the thin film and ±1 nm for the thick.

The values quoted in Sec. IV were derived first by finding the mean index at each wavelength point and then interpolating or extrapolating. For the thin film, since the values are quite far apart, a Cauchy expression was used for interpolation, but for the thick film only linear interpolation was used.

IV. Summary of Results and Discussion

Tables XVII and XVIII list the average thicknesses and optical constants of the Sc_2O_3 and Rh films obtained by the participating laboratories for the sample films prepared at OCLI (Sec. II). The tables also indicate the quantities measured and thin-film models used in the determinations. In addition, all groups assumed that the films were isotropic with plane-parallel boundaries and that they were deposited onto like substrates. They further assumed that the films and interfaces did not significantly scatter the incident radiation. This was established to be so by the Michelson Laboratory team (Sec. III.A). The final columns of the tables list the overall average values and variances of the thicknesses and optical constants.

The thicknesses of the films were determined by a variety of methods: by ellipsometry, with surface profilometers, by multiple-beam interferometry, from photometric and from spectrophotometric measurements. Only in the first two of the above methods is the thickness determined completely independently from the optical constants. Variation in thickness from one sample to another was expected to be negligible (Sec. II). OCLI's estimate that the thickness variation of the sample films was of the order of 0.5% was essentially confirmed by independent measurements at the Michelson Laboratory (0.7%) and at the University of New Orleans (0.4%).

The thicknesses of the Sc_2O_3 films determined by the different methods were remarkably close to the average values, 222.2 ± 3.9 and 451.5 ± 5.2 nm. Only the thicknesses determined by ellipsometry were somewhat higher, presumably because of the greater sensitivity of that method to inhomogeneities in the films. The remaining differences in the thicknesses can be explained by the variations in the refractive index: the variances of the determinations of the two thicknesses were 1.8 and 1.2 nm, and the average variance of the refractive-index determinations was 1.5%.

The average values of the Rh film thickness determinations were 15.5 ± 2.1 and 29.6 ± 2.2 nm. The agreement is satisfactory because these variances fall well within the 3.5-nm peak-to-valley roughness of the commercially polished fused silica substrates (Sec. III.A.)

In the determination of the optical constants of Sc_2O_3 many different models were assumed by the participating groups. Despite this, it will be seen from Table XVII that the agreement between the average refractive indices is remarkable—the mean variance for the 550–750-nm wavelength range is 0.01.

Although all groups saw evidence of the inhomogeneity of the Sc_2O_3 films, only three elected to measure the effect. A typical value of $(n_i - n_1)$ for $\lambda = 420$ nm is shown in Table XVII. The effect is quite significant, and the agreement between the three laboratories is good. More graphic representations will be found in Figs. 4, 5, and 7. From these it will be seen that the inhomogeneity is both thickness and wavelength dependent. This latter fact is difficult to explain, and it may indicate that an even more complicated model might be needed to explain fully the behavior of the Sc_2O_3 films.

Table XVII. Summary of the Results for Sc_2O_3 Films

Section	3A	3B	3C	3D	3E	3F	3H	
Institution	Michelson Laboratory	University of New Orleans	Centre d'Etudes des Couches Minces	Optical Coating Laboratory Inc.	Vought Corporation	National Research Council of Canada	Optical Sciences Center	
Method	R, T and t	Reflection Ellipsometry	Wide-Band Spectrophotometric	Modified Valeev Turning Point	Algebraic Inversion	Inverse Synthesis	Envelope	
Measurement quantities	R, T, t for single λ's	ψ_{60}, Δ_{60} for single λ's	R, T for many λ's	T_{max}, T_{min}, R_{min}	R, T, t for single λ's	R, T, $T_p(45)$, $T_s(45)$, $T_p(60)$, $T_s(60)$. T^* for many λ's	T_{max}, R_{max} T_{min}, R_{min}	Mean values and variances
t_1 (nm)	224.5	228.2	217.6	219.0	225.0	221.2	219.4	222.2±3.9
t_2 (nm)	452.5	462.6	447.8	447.4	450.0	450.3	449.6	451.5±5.2
Thin film model differences	nonabsorbing, homogeneous films	absorbing, homogeneous; n same for both films	nonabsorbing, linearly inhomogeneous films	absorbing, linearly inhomogeneous films	nonabsorbing, homogeneous films	absorbing, homogeneous; n same for both films	weakly absorbing, linearly inhomogeneous films	
λ(nm)	n	n‡	n	n‡	n	n	n‡	n
400 t_1	—	2.07	1.89	1.91	—	1.87	1.90	1.93
400 t_2	—		1.89	1.90	—		1.89	±0.08
450 t_1	1.70	2.01	1.88	1.89	1.84	1.86	1.88	1.88
450 t_2	1.86		1.87	1.88	1.87		1.89	±0.07
500 t_1	1.86	1.93	1.87	1.88	—	1.85	1.86	1.87
500 t_2	1.85		1.86	1.87	1.86		1.87	±0.03
550 t_1	1.84	1.85	1.87	1.86	1.87	1.85	1.85	1.86
550 t_2	1.87		1.85	1.85	—		1.86	±0.01
600 t_1	1.84	1.82	1.87	1.85	1.84	1.84	1.83	1.84
600 t_2	1.86		1.85	1.84	1.87		1.85	±0.02
650 t_1	1.84	1.81	1.86	1.84	1.82	1.84	1.82	1.83
650 t_2	1.82		1.84	1.83	1.82		1.84	±0.01
700 t_1	1.83	—	1.86	1.84	1.81	1.84	1.81	1.83
700 t_2	1.84		1.84	1.83	1.83		1.83	±0.01
750 t_1	1.82	—	—	1.83	—	1.84	—	1.83
750 t_2	1.84		—	1.82	—		—	±0.01
(n_i-n_1) t_1 at λ=420			0.15	0.17			0.17	
(n_i-n_1) t_2 at λ=420			0.18	0.20			0.20	

‡ Interpolated values.

Table XVIII. Summary of the Results for Rh Films

Section	3A		3B		3D		3E		3F		3G		
Institution	Michelson Laboratory		University of New Orleans		Optical Coating Laboratory Inc.		Vought Corporation		National Research Council of Canada		Optical Sciences Center		
Method	R, T and t Method		Reflection Ellipsometry		Nestell and Christy		Algebraic Inversion		Inverse Synthesis		Bennett and Booty		
Measurement quantities	R, T, t for single λ's		ψ_{60}, Δ_{60} for single λ's		T, R, $T_p(60)$ for single λ's		R, T, t for single λ's		R, T, $T_p(45)$, $T_s(45)$, $T_p(60)$, $T_s(60)$, T_T for many λ's		R, T, t, R' for single λ's		Mean values and variances
t_1 (nm)	14.2		15.5		17.2		12.0		16.9		17.0		15.5±2.1
t_2 (nm)	27.1		31.6		30.1		27.5		31.7		—		29.6±2.2
Thin film model differences	homogeneous films		homogeneous; same n, k for both films		homogeneous films		homogeneous films		homogeneous; same n, k for both films		homogeneous films		
λ(nm)	n	k	n‡	k‡	n	k	n	k	n	k	n	k	n	k
400 t_1	—	—	2.10	3.00	1.86	2.88	2.50	3.45	1.80	2.85	3.16	2.15	2.18	2.91
t_2	—	—			1.86	2.97	2.40	3.00			—	—	±0.45	±0.34
450 t_1	2.40	3.29	2.35	3.12	2.04	3.02	2.75	3.55	2.11	3.00	3.19	2.34	2.38	3.08
t_2	2.27	3.25			1.96	3.12	2.75	3.15			—	—	±0.38	±0.29
500 t_1	2.60	3.40	2.56	3.25	2.18	3.14	3.10	3.55	2.20	3.15	3.22	2.54	2.55	3.21
t_2	2.39	3.42			2.04	3.27	3.00	3.15			—	—	±0.40	±0.26
550 t_1	2.78	3.53	2.74	3.41	2.32	3.28	3.20	3.75	2.40	3.25	3.19	2.79	2.68	3.36
t_2	2.51	3.58			2.13	3.43	3.10	3.30			—	—	±0.37	±0.24
600 t_1	2.95	3.65	2.92	3.54	2.46	3.40	3.30	3.90	2.55	3.35	3.15	3.03	2.81	3.50
t_2	2.62	3.75			2.23	3.59	3.30	3.40			—	—	±0.36	±0.23
650 t_1	3.11	3.77	3.08	3.68	2.61	3.52	3.35	4.15	2.75	3.50	3.13	3.26	2.94	3.65
t_2	2.75	3.89			2.36	3.74	3.35	3.50			—	—	±0.32	±0.24
700 t_1	3.23	3.91	—	—	2.75	3.63	3.60	4.20	2.90	3.60	3.07	3.47	3.03	3.77
t_2	2.87	4.04			2.47	3.88	3.50	3.60			—	—	±0.36	±0.25
750 t_1	3.35	4.03	—	—	2.88	3.74			3.00	3.75	3.07	3.61	2.99	3.86
t_2	3.01	4.16			2.60	4.01					—	—	±0.22	±0.20

‡ Interpolated values.

Five groups made separate determinations of the average refractive indices of the thin and thick Sc_2O_3 films. The difference between these two refractive indices is much smaller than $(n_i - n_1)$. It is of the same order of magnitude as the mean variance of the refractive-index determinations and was either negative or positive.

Some participating groups assumed at the outset that the Sc_2O_3 films were nonabsorbing. Those who did not found that the absorption coefficient of the Sc_2O_3 films was so small that their methods were not able to yield significant values for it. Should it be important to measure this quantity, different methods must be employed, such as those based on calorimetry or on attenuation in lightguides.

The results of the determinations of the optical constants of the Rh films are less satisfactory. The average variances of the determinations of n,k in the 400–750-nm spectral region were 0.35, 0.26, respectively. Expressed in percent, the variances are 13 and 8%. Furthermore, these results differ greatly from published data.

Probably many factors contribute to this situation. It is possible that some of the determinations did not converge to the right values. As a rule, metal films are less stable than oxide layers. There is evidence that some oxidation and aging of the films occurred (Secs. III.A,III.D,III.E). It is possible that after the preparation the Rh samples aged differently and that some of the differences in the values are real. The aging and oxidation may have given rise to a surface layer and/or an inhomogeneous film. Yet all the thin-film models in the present determinations assumed the existence of a single homogeneous film. It is likely that departures from this simple model will have different effects on different methods for the determination of n and k. Another contributing factor may have been the low percentage accuracy (14 and 7%) of the determination of the thicknesses of the Rh films. For example, the determination of the absorption coefficient often depends strongly on the accuracy of the thickness determination. Evidence that this may be so in the present case is the fact that the products kt are more constant than either k or t alone.

It is very likely that different starting materials and preparation conditions contributed to the large departure of the optical constants published in this paper from those in previous work.[5]

The Michelson Laboratory team would like to thank D. L. Decker for helping design and build the laser apparatus to measure reflectance and transmittance and P. C. Archibald for making the scattering measurements on the Sc_2O_3 films.

The work of Azzam and Thonn was supported by the State of Louisiana Board of Regents and the National Science Foundation.

The OCLI team wishes to acknowledge the work of R. H. Miller in implementing the method of Valeev at OCLI and the work of B. Vidal for writing the computer program code used for the Nestell-Christy method.

The NRCC team would like to thank P. Brennan, R. Simpson, and A. Waldorf who took the measurements.

U. J. Gibson and R. Swenson wish to acknowledge H. G. Craighead, who developed the computer code from which the program used here was derived.

References

1. J. M. Bennett, "Optical Evaluation Techniques for Thin Films," J. Opt. Soc. Am. **73,** 1865A (1983).
2. H. K. Pulker, "Mechanical Characterization of Optical Films," J. Opt. Soc. Am. **73,** 1865A (1983).
3. D. E. Gray, Ed., *American Institute of Physics Handbook* (McGraw-Hill, New York, 1972), p. 6–28 (refractive index of fused silica); p. 6–120 (equations for calculating n and k from T_f, R_f, and film thickness).
4. F. Rainer, W. H. Lowdermilk, D. Milam, T. Tuttle Hart, T. L. Lichtenstein, and C. K. Carniglia, "Scandium Oxide Coatings for High-Power UV Laser Applications," Appl. Opt. **21,** 3685 (1982).
5. J. K. Coulter, G. Hass, and J. B. Ramsey, Jr., "Optical Constants of Rh Films in Visible," J. Opt. Soc. Am. **63,** 1149 (1973).
6. D. L. Decker, in *Laser Induced Damage in Optical Materials: 1975*, A. J. Glass and A. H. Guenther, Eds., NBS Spec. Publ. 435 (Apr. 1976), pp. 230–235.
7. H. E. Bennett and J. L. Stanford, "Structure-Related Optical Characteristics of Thin Metallic Films in the Visible and Ultraviolet," J. Res. Natl. Bur. Stand. Sect. A **80,** 643 (1976).
8. J. M. Bennett and J. H. Dancy, "Stylus Profiling Instrument for Measuring Statistical Properties of Smooth Optical Surfaces," Appl. Opt. **20,** 1785 (1981).
9. J. M. Bennett, "Measurement of the rms Roughness, Autocovariance Function, and Other Statistical Properties of Optical Surfaces Using a FECO Scanning Interferometer," Appl. Opt. **15,** 2705 (1976).
10. H. E. Bennett, "Scattering Characteristics of Optical Materials," Opt. Eng. **17,** 480 (1978); P. C. Archibald and H. E. Bennett, "Scattering from Infrared Missile Domes," Opt. Eng. **17,** 647 (1978).
11. H. E. Bennett and J. M. Bennett, in *Physics of Thin Films, Vol. 4*, G. Hass and R. E. Thun, Eds. (Academic, New York, 1967), pp. 1–96 (see especially pp. 42–44, "Transmittance of a Thin Film on a Nonabsorbing Substrate").
12. R. M. A. Azzam and N. M. Bashara, *Ellipsometry and Polarized Light* (North-Holland, Amsterdam, 1977).
13. Ref. 12, Secs. 3.7 and 5.4.
14. I. H. Malitson, "Refractive Index of Fused Silica," J. Opt. Soc. Am. **55,** 1205 (1965).
15. R. M. A. Azzam, A.-R. M. Zaghloul and N. M. Bashara, "Ellipsometric Function of a Film–Substrate System: Applications to the Design of Refraction-type Optical Devices and to Ellipsometry," J. Opt. Soc. Am. **65,** 252 (1975).
16. J. P. Borgogno, B. Lazarides, and E. Pelletier, "Automatic Determination of the Optical Constants of Inhomogeneous Thin Films," Appl. Opt. **21,** 4020 (1982).
17. J. P. Borgogno and B. Lazarides, "An Improved Method for the Determination of the Extinction Coefficient of Thin Film Materials," Thin Solid Films **102,** 209 (1983).
18. E. Pelletier, P. Roche, and B. Vidal, "Détermination Automatique des Constantes Optiques et de l'Épaisseur des Couches Minces: Application aux Couches Diélectriques," Nouv. Rev. Opt. **7,** 353 (1976).
19. J. Strong, *Procedures in Experimental Physics* (Prentice-Hall, Englewood Cliffs, N.J., 1963), p. 376.
20. A. Savitsky and M. J. E. Golay, "Smoothing and Differentiation

of Data by Simplified Least Squares Procedures," Anal. Chem. **36**, 1627 (1964).
21. A. S. Valeev, "Determination of the Optical Constants of Weakly Absorbing Thin Films," Opt. Spectrosc. USSR **15**, 269 (1963).
22. A. S. Valeev, "Constants of Thin Weakly Absorbing Lasers," Opt. Spectrosc. USSR **18**, 498 (1965).
23. J. E. Nestell, Jr., and R. W. Christy, "Derivation of Optical Constants of Metals from Thin-Film Measurements at Oblique Incidence," Appl. Opt. **11**, 643 (1972).
24. C. K. Carniglia and B. Vidal, "Optical Constants of Oxidized Thin Metal Films," J. Opt. Soc. Am. **71**, 1554 (1981).
25. W. E. Case, "Algebraic Method for Extracting Thin-Film Optical Parameters from Spectrophotometer Measurements," Appl. Opt. **22**, 1832 (1983); Also, W. E. Case and M. K. Purvis, "Method for Synthesis of Optical Thin-Film Coatings on Small Computers," J. Opt. Soc. Am. **73**, 1879A (1983).
26. S. Tolansky, *Multiple-Beam Interferometry of Surfaces and Films* (Clarendon, Oxford, 1983).
27. J. A. Dobrowolski, F. C. Ho, and A. Waldorf, "Determination of Optical Constants of Thin Film Coating Materials Based on Inverse Synthesis," Appl. Opt. **22**, 3191 (1983).
28. J. M. Bennett, and M. J. Booty, "Computational Method for Determining n and k for a Thin Film from the Measured Reflectance, Transmittance, and Film Thickness," Appl. Opt. **5**, 41 (1966).
29. M. Born and E. Wolf, *Principles of Optics* (Pergamon, Oxford, 1983), p. 55.
30. J. C. Manifacier, J. Gasiot, and J. D. Fillard, "A Simple Method for the Determination of the Optical Constants n_1k and the Thickness of a Weakly Absorbing Thin Film," J. Phys. E **9**, 1002 (1976).

Meeting Reports *continued from page 3523*

of the $A^2\Pi$-$X^2\Sigma$ transition of CaOH using a single mode ring dye laser to determine accurate rotational constants which will be employed in a microwave search for interstellar CaOH, and a tunable infrared diode laser study of Fermi and Coriolois interactions in the CH_3I vs. fundamental. Kinetics measurements of the potential chemical laser reaction $Sn(^3pj) + N_2O \rightarrow SnO^* + N_2$ by *Wang Xiuyan* [Luda (Darien) Institute of Chemical Physics] and co-workers found that the $Sn(^3p_1)$ spin-orbit state reacted eight times faster than the $Sn(^3p_{0,2})$ states. This work was performed in a high temperature fast flow reactor (HTFR) and also yielded spectroscopic constants for five lowest lying spectroscopic states $X^1\Sigma^+$, a $3\Sigma^+$, b, b', and $A^1\Sigma^+$. It was noted that Ar quenched the a state more efficiently than the b state.

A paper on the laser and optical probing of the crossed molecular beam reactions of $Ba(^1S$ and $^3D)$ with CH_nCl_{4-n} (n = 0,1,2) and $C_2H_{6-n}Cl_n$ (n = 2,3,4) was presented by *Dong Linna* and co-workers [Luda (Darien) Institute of Chemical Physics]. LIF of the BaCl $C^2\Pi_2$-$X^2\Sigma^+$ system was used to probe the BaCl $X^2\Sigma^+$ product. The results indicated a very low yield from the $Ba(^3D) + CCl_4$ reaction. Chemiluminescence spectra of CCl_2(A-X) and BaCl($A^2\Pi$,$B^2\Sigma^+C^2\Pi$) were observed in the $Ba(^3D) + CCl_4$ reactions. In general, their results showed much lower yields of chemiluminescent products from reactions of $Ba(^1S)$ relative to $BA(^3D)$.

Shen Zhongxin (Fudan University) reported the formation of Pt, Au, and Mo silicides by irradiating P = type Si(111) coated with 400 → 5700 Å thick films of the metals (+ZrO_2 AR coating) using a Q-switched Nd:YAG laser (1.0 kW at 532 nm, 50 μm spot size). In work performed at EPFL Switzerland, *Qiu Mingxin* (Shanghai Institute of Laser Technology) used the 454.5, 514.5 (and 257.3) nm Ar^+ lines for photo- and pyrodeposition of Sn and Pt onto carbon or quartz surfaces. The ultimate resolution obtained was 0.2 μm. In a poster paper, *Li Fuming* and co-workers reported the Ar^+ laser enhanced etching of GaAs and Si substrates (both doped and undoped) using liquids etchants (KOH,H_2SO_4-H_2O_2,H_3PO_4-H_2O_2). Most of the effects were attributed to thermal mechanisms with 50 to 100 μ/min etch rates. However, direct photo enhancement was observed for GaAs/H_2SO_4=H_2O_2.

Harmonic generation and sum frequency mixing in an organic crystal, L-arginine phosphate, was reported by *Zhongke* and co-workers (Institute of Crystal Materials, Shandong University). The crystal has good UV transmission and large optical nonlinear coefficients. The SHG efficiency was 3.5 times greater than that of KDP for 0.532 μm radiation.

The general impression of this participant was that much of the Chinese work presented at this conference indicated notable progress in areas previously established in the non-Chinese literature. The research areas where the Chinese community appears to be making its strongest impact is in materials development (particularly rare-earth containing compounds) and low power clinical applications of lasers.

This report is reprinted from *Scientific Bulletin April–June 1984*, Vol. **9**, No. 2, a publication of the Department of Navy Office of Naval Research Far East and the Department of Air Force Office of Scientific Research Far East.